

MOLECULAR SPECTROSCOPY (19PPH10)

UNIT – I

Infrared Spectroscopy

Principle and theory of Infrared spectroscopy – Far and Near IR absorption spectroscopy – Mid and Near IR reflectance spectroscopy- Photo acoustic IR spectroscopy – Dispersive IR spectrometer – IR Imaging – FTIR spectroscopy – Vibrational frequencies and qualities analysis – sampling methods – Instrumentation- Applications.

PRINCIPLE AND THEORY OF IR SPECTROSCOPY:

Infrared (IR) spectroscopy or vibrational spectroscopy is an analytical technique that takes advantage of the vibrational transitions of a molecule.

It is one of the most common and widely used spectroscopic techniques employed mainly by inorganic and organic chemists due to its usefulness in determining structures of compounds and identifying them.

The method or technique of infrared spectroscopy is conducted with an instrument called an infrared spectrometer (or spectrophotometer) to produce an infrared spectrum.

Principle of IR

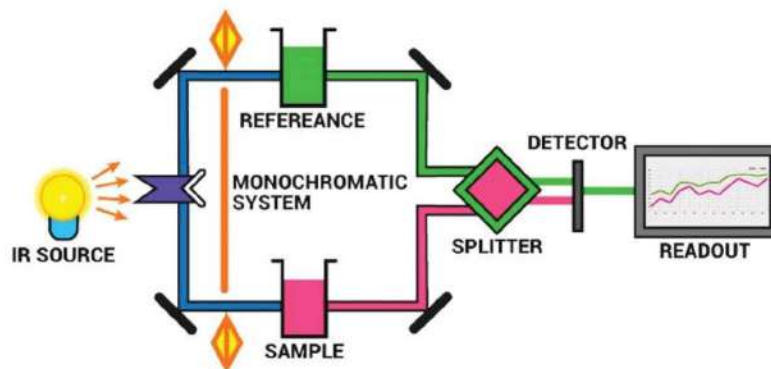
1. Infrared Spectroscopy is the analysis of infrared light interacting with a molecule.
2. The portion of the infrared region most useful for analysis of organic compounds have a wavelength range from 2,500 to 16,000 nm, with a corresponding frequency range from 1.9×10^{13} to 1.2×10^{14} Hz.

3. Photon energies associated with this part of the infrared (from 1 to 15 kcal/mole) are not large enough to excite electrons, but may induce vibrational excitation of covalently bonded atoms and groups.
4. It is known that in addition to the facile rotation of groups about single bonds, molecules experience a wide variety of vibrational motions, characteristic of their component atoms.
5. Consequently, virtually all organic compounds will absorb infrared radiation that corresponds in energy to these vibrations.
6. Infrared spectrometers, similar in principle to other spectrometer, permit chemists to obtain absorption spectra of compounds that are a unique reflection of their molecular structure.
7. The fundamental measurement obtained in infrared spectroscopy is an infrared spectrum, which is a plot of measured infrared intensity versus wavelength (or frequency) of light.
8. IR Spectroscopy measures the vibrations of atoms, and based on this it is possible to determine the functional groups.
9. Generally, stronger bonds and light atoms will vibrate at a high stretching frequency (wavenumber).

Instrumentation of IR

The main parts of IR spectrometer are as follows:

1. Radiation source
2. Sample cells and sampling of substances
3. Monochromators
4. Detectors
5. Recorder



1. IR Radiation Source

IR instruments require a source of radiant energy which emit IR radiation which must be steady, intense enough for detection and extend over the desired wavelength.

Various sources of IR radiations are as follows.

1. Nernst glower
2. Incandescent lamp
3. Mercury arc
4. Tungsten lamp
5. Glycer source
6. Nichrome wire

2. Sample cells and sampling of substances

IR spectroscopy has been used for the characterization of solid, liquid or gas samples.

i. Solid – Various techniques are used for preparing solid samples such as pressed pellet technique, solid run in solution, solid films, mull technique etc.

ii. Liquid – Samples can be held using a liquid sample cell made of alkali halides. Aqueous solvents cannot be used as they will dissolve alkali halides. Only organic solvents like chloroform can be used.

iii. Gas– Sampling of gas is similar to the sampling of liquids.

3. Monochromators

1. Various types of monochromators are prism, gratings and filters.
2. Prisms are made of Potassium bromide, Sodium chloride or Caesium iodide.
3. Filters are made up of Lithium Fluoride and Diffraction gratings are made up of alkali halides.

4. Detectors

1. Detectors are used to measure the intensity of unabsorbed infrared radiation.
2. Detectors like thermocouples, Bolometers, thermistors, Golay cell, and pyro-electric detectors are used.

5. Recorder

Recorders are used to record the IR spectrum.

Applications of IR

It has been of great significance to scientific researchers in many fields such as:

- Protein characterization
- Nanoscale semiconductor analysis and
- Space exploration.
- Analysis of gaseous, liquid or solid samples
- Identification of compounds
- Quantitative analysis

- Information regarding functional groups of molecules and constitution of molecules can be deduced from IR spectrum
- To know about interaction among molecules

Near Infrared (NIR)

Near infrared (NIR) light therapy is a form of photobiomodulation that uses invisible, near-infrared wavelengths between 700 and 1200nm³ (nanometers) to deliver energy to cells. Scientific research shows that when delivered at the vital wavelength of 880nm, without extreme heat or light. [5] The wavelength of Near Infrared is the shortest of the three infrareds.

It's absorbed just below the surface of the skin, promoting wound healing, cell health/regeneration, skin revitalization and can mitigate inflammation. NIR has also been shown to help clear up acne lesions, improve fine lines and wrinkles, and encourages collagen synthesis . It promotes skin renewal, cell health, wound healing, and tissue growth.

Mid Infrared (MIR)

Compared to near infrared wavelengths (which effectively penetrate and heal the skin) and far infrared wavelengths (which reach deep into the body, where toxins are stored), mid infrared wavelengths are longer than NIR, thus allowing for greater penetration into soft tissue. [5] MIR can help with inflammation, pain and decrease overall healing time. Other benefits of infrared sauna include weight loss and the expansion of blood vessels, which leads to improved circulation

MIR helps expand blood vessels and increases circulation so more oxygen can reach injured areas of the body. This reduces pain and speeds the healing process.

When used in combination with far infrared waves, MIR effectively stimulates the cardiovascular system and raises body temperature. As the body works to cool itself, heart rate, cardiac output and metabolic rate increase as they do during exercise. This in turn supports weight loss.

Far Infrared (FIR)

Being the longest wavelength, FIR penetrates the deepest where toxins and chemicals can be trapped. It can assist with weight loss and increases your heart rate. This increase in BPM's can be equivalent to a mild cardio workout.

In addition, FIR stimulates vasodilation, which in turn increases blood flow throughout the body. FIR can also reduce pain, ease joint stiffness, decrease inflammation and alleviate overall body stress. And of course powerfully detox you through substantial perspiration.

In conclusion, Near, Mid, and Far infrared waves penetrate the skin, muscles, joints, and tissues to increase circulation, speed oxygen flow, and help rid the body of harmful toxins.

They also help to remove impurities from your cells, specifically the cells inside our fat where our body stores waste and harmful toxins such as cholesterol and heavy metals.

Region of IR	Wave length (μm)	Wave number (cm^{-1})
Near IR (Overtone region)	0.8-2.5	12,500-4000
Mid IR (Vibration- rotation region)	2.5-50	4000-200
Far IR (Rotation region)	50-1000	200-10
Most used	2.5-25	4000-400

PHOTOACOUSTIC SPECTROSCOPY:

It is the measurement of the effect of absorbed electromagnetic energy (particularly of light) on matter by means of acoustic detection. The discovery of the photoacoustic effect dates to 1880 when Alexander Graham Bell showed that thin discs emitted sound when exposed to a beam of sunlight that was rapidly interrupted with a rotating slotted disk. The absorbed energy from the light causes local heating and through thermal expansion a pressure wave or sound. Later Bell showed that materials exposed to the non-visible portions of the solar spectrum (i.e., the infrared and the ultraviolet) can also produce sounds.

A photo acoustic spectrum of a sample can be recorded by measuring the sound at different wavelengths. This spectrum can be used to identify the absorbing components of the sample. The photo acoustic effect can be used to study solids, liquids and gases.

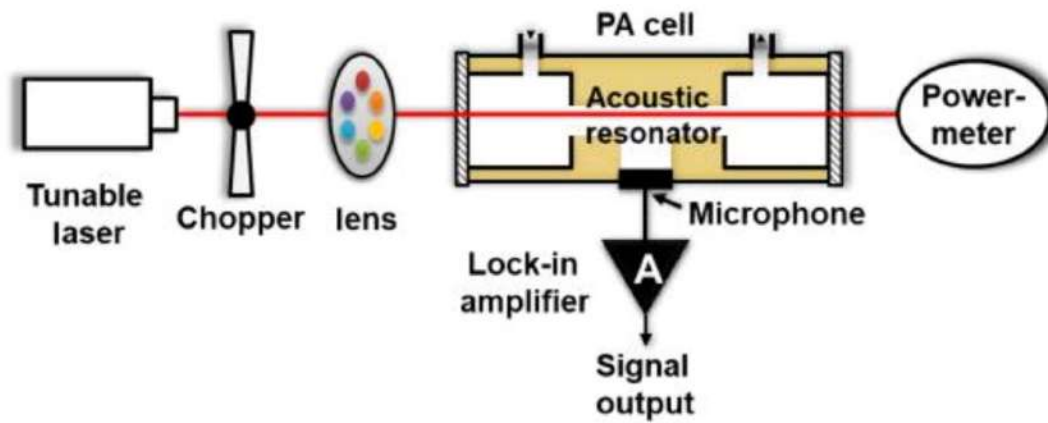


Photo acoustic spectroscopy has become a powerful technique to study concentrations of gases at the part per billion or even part per trillion levels.^[2] Modern photo acoustic detectors still rely on the same principles as Bell's apparatus; however, to increase the sensitivity, the following modifications have been made:

Use of intense lasers instead of the sun to illuminate the sample since the intensity of the generated sound is proportional to the light intensity; this technique is referred to as "laser photo acoustic spectroscopy" or "LPAS"^[2]

The ear has been replaced by sensitive microphones. The microphone signals are further amplified and detected using lock-in amplifiers.

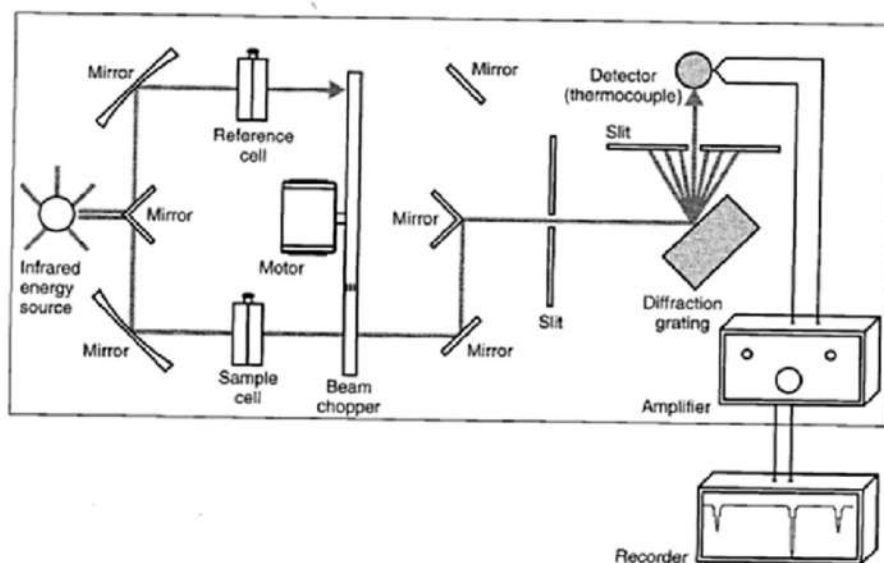
By enclosing the gaseous sample in a cylindrical chamber, the sound signal is amplified by tuning the modulation frequency to an acoustic resonance of the sample cell.

DISPERSIVE IR SPECTROMETER:

These are often double-beam recording instruments, employing diffraction gratings for dispersion of radiation.

Radiation from the source is flicked between the reference and sample paths. Often, an optical null system is used. This is when the detector only responds if the intensity of the two beams is unequal. If the intensities are unequal, a light attenuator restores equality by moving in or out of the reference beam. The recording pen is attached to this attenuator.

Working



Dispersive spectrometers generate spectra by optically *dispersing* the incoming radiation into its frequency or *spectral* components, as illustrated in the figure below. Common dispersive elements include prisms and gratings. Dispersive spectrometers can be further classified into two types: monochromators and spectrographs.

A monochromator uses a single detector, narrow slit(s) (usually two, one at the entrance and another at the exit port), and a rotating dispersive element allowing the user to observe a selected range of wavelength. The figure below shows the simplified schematic of a monochromator.

A spectrograph, on the other hand, uses an array of detector elements and a stationary dispersive element. In this case, the slit shown in the figure is removed, and spectral elements over a wide range of wavelengths are obtained at the same time, therefore providing faster measurements with a more expensive detection system

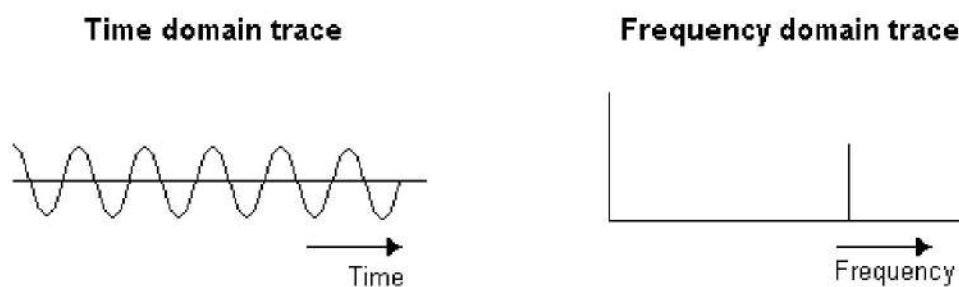
Applications

- A spectrometer is a tool for determining wavelengths of light over a wide variety of electromagnetic spectrum.
- It is commonly utilized for spectroscopic analysis of sample materials.
- The incident light from the light source can be transmitted, soaked up, or mirrored through the sample.
- The changes that occur throughout the interaction of incident light with the sample show the features and characteristics of samples

FOURIER-TRANSFORM SPECTROMETERS:

FTIR Analysis measures the infrared region of the electromagnetic radiation spectrum, which has a longer wavelength and a lower frequency than visible light, and is measurable in a sample when submitted to infrared radiation (IR). The basic theory at work is that the bonds between different elements absorb light at different frequencies.

The light is measured using an infrared spectrometer which produces the output of an infrared spectrum. The IR spectrum is a graph of infrared light absorbance by the substance on the vertical axis and the frequency (wavelength) on the horizontal axis. Any waveform can be shown in one of two ways; either in frequency domain or time domain.



Dispersive IR instruments operate in the frequency domain. There are, however, advantages to be gained from measurement in the time domain followed by computer transformation into the frequency domain.

If we wished to record a trace in the time domain, it could be possible to do so by allowing radiation to fall on a detector and recording its response over time. In practice, no detector can respond quickly enough (the radiation has a frequency greater than 10^{14} Hz). This problem can be solved by using interference to modulate the i.r. signal at a detectable frequency. The Michelson interferometer is used to produce a new signal of a much lower frequency which contains the same information as the original IR signal. The output from the interferometer is an interferogram.

INSTRUMENTATION:

SOURCES:

An inert solid is electrically heated to a temperature in the range 1500-2000 K. The heated material will then emit infra red radiation.

THE NERNST GLOWER :

It is a cylinder (1-2 mm diameter, approximately 20 mm long) of rare earth oxides. Platinum wires are sealed to the ends, and a current passed through the cylinder. The Nernst glower can reach temperatures of 2200 K.

THE GLOBAL SOURCE:

It is a silicon carbide rod (5mm diameter, 50mm long) which is electrically heated to about 1500 K. Water cooling of the electrical contacts is needed to prevent arcing. The spectral output is comparable with the Nernst glower, except at short wavelengths (less than 5 mm) where it's output becomes larger.

THE INCANDESCENT WIRE SOURCE:

It is a tightly wound coil of nichrome wire, electrically heated to 1100 K. It produces a lower intensity of radiation than the Nernst or Global sources, but has a longer working life.

DETECTORS:

There are three categories of detector;

Thermal

Pyroelectric

Photo conducting

THERMOCOUPLES:

Consist of a pair of junctions of different metals; for example, two pieces of bismuth fused to either end of a piece of antimony. The potential difference (voltage) between the junctions changes according to the difference in temperature between the junctions.

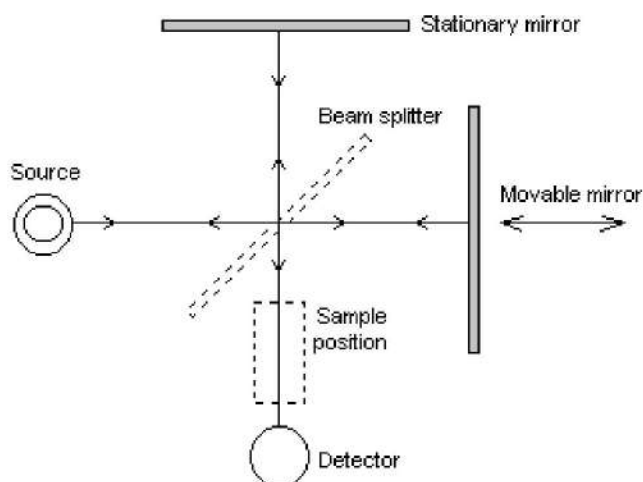
PYROELECTRIC DETECTORS:

Are made from a single crystalline wafer of a pyroelectric material, such as triglycerine sulphate. The properties of a pyroelectric material are such that when an electric field is applied across it, electric polarisation occurs (this happens in any dielectric material). In a pyroelectric material, when the field is removed, the polarisation persists. The degree of polarisation is temperature dependant. So, by sandwiching the pyroelectric material between two electrodes, a temperature dependant capacitor is made. The heating effect of incident IR radiation causes a change in the capacitance of the material. Pyroelectric detectors have a fast response time. They are used in most Fourier transform IR instruments.

PHOTOELECTRIC DETECTORS:

Such as the mercury cadmium telluride detector comprise a film of semiconducting material deposited on a glass surface, sealed in an evacuated envelope. Absorption of IR promotes nonconducting valence electrons to a higher, conducting, state. The electrical resistance of the semiconductor decreases. These detectors have better response characteristics than pyroelectric detectors and are used in FT-IR instruments - particularly in GC - FT-IR.

Working



FTIR analysis measures the range of wavelengths in the infrared region that are absorbed by a material. This is accomplished through the application of infrared radiation (IR) to samples of a material. The sample's absorbance of the infrared light's energy at various wavelengths is measured to determine the material's molecular composition and structure.

Unknown materials are identified by searching the spectrum against a database of reference spectra. Materials can be quantified using the FTIR materials characterization technique as long as a standard curve of known concentrations of the component of interest can be created.

FTIR Analysis can be used to identify unknown materials, additives within polymers, surface contamination on a material, and more. The results of the tests can pinpoint a sample's molecular composition and structure. A simple device called an interferometer is used to identify samples by producing an optical signal with all the IR frequencies encoded into it. The signal can be measured quickly.

Then, the signal is decoded by applying a mathematical technique known as Fourier transformation. This computer-generated process then produces a mapping of the spectral information. The resulting graph is the spectrum which is then searched against reference libraries for identification. With the microscope attachment, samples as small as 20 microns can be analyzed. This allows quick and cost effective identification of unknown particles, residues, films or fibers. FTIR testing can also measure levels of oxidation in some polymers or degrees of cure in other polymers as well as quantifying contaminants or additives in materials.

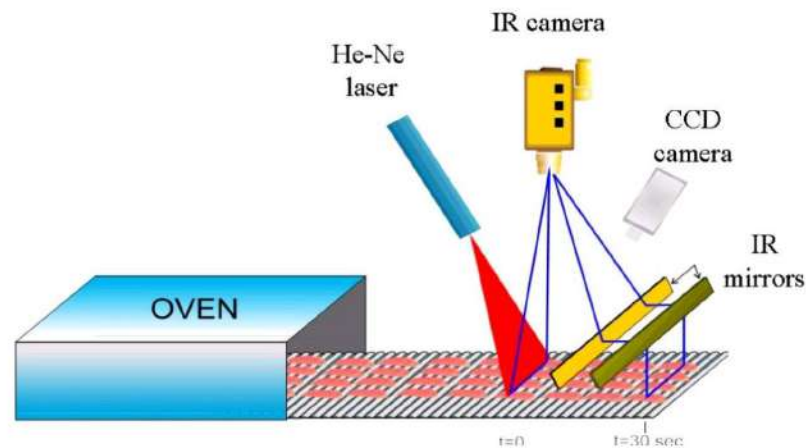
ADVANTAGES OF FOURIER TRANSFORM IR OVER DISPERSIVE IR:

1. Improved frequency resolution
2. Improved frequency reproducibility (older dispersive instruments must be recalibrated for each session of use)
3. Higher energy throughput
4. Faster operation
5. Computer based (allowing storage of spectra and facilities for processing spectra)
6. Easily adapted for remote use (such as diverting the beam to pass through an external cell and detector, as in GC - FT-IR)

IR IMAGING:

Foodborne diseases caused by undercooked poultry products are noteworthy problems that have motivated research into the assessment of the endpoint temperature in meat. In this research, a novel infrared and laser range

imaging system was proposed to estimate the internal cooking temperature of chicken breasts. It consisted of three subsystems: an IR imaging system, a laser range system, and an artificial neural network modeling system.

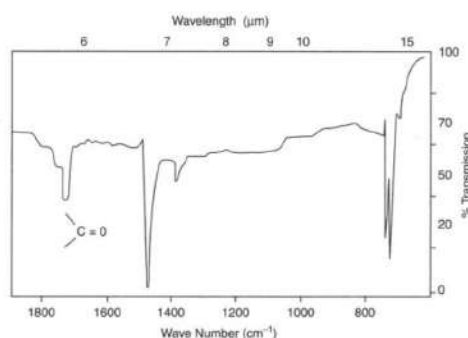


VIBRATIONAL FREQUENCIES AND QUALITIES ANALYSIS:

IR spectroscopy is a great method for identification of compounds, especially for identification of functional groups. Therefore, we can use group frequencies for structural analysis. Group frequencies are vibrations that are associated with certain functional groups. It is possible to identify a functional group of a molecule by comparing its vibrational frequency on an IR spectrum to an IR stored data bank.

Here, we take the IR spectrum of Formaldehyde for an example. Formaldehyde has a C=O functional group and C-H bond. The value obtained from the following graph can be compared to those in reference data banks stored for Formaldehyde. A molecule with a C=O stretch has an IR band which is usually found near 1700cm^{-1} and around 1400cm^{-1} for CH_2 bend. It's important to note that this value is dependent on other functional groups present on the molecule.

The higher 1700cm^{-1} indicates a large dipole moment change. It is easier to bend a molecule than stretch it, hence stretching vibrations have higher frequencies and require higher energies than bending modes. The finger print region is a region from $1400\text{-}650\text{ cm}^{-1}$. Each molecule has its own characteristic print and is often cumbersome to attach any values to this region.



QUANTITATIVE ANALYSIS:

Infrared spectroscopy can also be applied in the field of quantitative analysis, although sometimes it's not as accurate as other analytical methods, like gas chromatography and liquid chromatography. The main theory of IR quantification is Beer's law or Beer-Lambert law, which is written as

$$A = \log(I_0/I) = \epsilon lc$$

Where A is the absorbance of the sample, I is the intensity of transmitted light, I_0 is the intensity of incident light, l is the path length, ϵ is the molar absorptivity of the substance, and c is the concentration of the substance.

From the Beer's Law, we could figure out the relation between the absorbance and the concentration of the sample since the analytes have a particular molar absorptivity at a particular wavelength. Therefore, we could use

IR spectroscopy and Beer's Law to find the concentration of substance or the components of mixture. This is how the IR quantification operated.

SAMPLING METHODS:

IR spectroscopy is used for the characterization of solid, liquid or gas samples. Material containing sample must be transparent to the IR radiation. So, the salts like NaCl, KBr are only used.

1. SAMPLING OF SOLIDS:

Various techniques used for preparing solid samples are as follows

a) Mull technique: In this technique, the finely crushed sample is mixed with Nujol (mulling agent) in a marble or agate mortar, with a pestle to make a thick paste. A thin film is applied onto the salt plates. This is then mounted in a path of IR beam and the spectrum is recorded.

b) Solid run in Solution – In this technique, solid sample may be dissolved in a non-aqueous solvent provided that there is no chemical interaction with the solvent and the solvent is not absorbed in the range to be studied. A drop of solution is placed on the surface of alkali metal disc and solvent is evaporated to dryness leaving a thin film of the solute.

c) Case film technique – If the solid is amorphous in nature then the sample is deposited on the surface of a KBr or NaCl cell by evaporation of a solution of the solid and ensured that the film is not too thick to pass the radiation.

d) Pressed pellet technique – In this technique, a small amount of finely ground solid sample is mixed with 100 times its weight of potassium bromide and

compressed into a thin transparent pellet using a hydraulic press. These pellets are transparent to IR radiation and it is used for analysis.

2. SAMPLING OF LIQUIDS:

Liquid sample cells can be sandwiched using liquid sample cells of highly purified alkali halides, normally NaCl. Other salts such as KBr and CaF₂ can also be used. Aqueous solvents cannot be used because they cannot dissolve alkali halides. Organic solvents like chloroform can be used. The sample thickness should be selected so that the transmittance lies between 15-20%. For most liquids, the sample cell thickness is 0.01-0.05 mm. Some salt plates are highly soluble in water, so the sample and washing reagents must be anhydrous

3. SAMPLING OF GASES:

The sample cell is made up of NaCl, KBr etc. and it is similar to the liquid sample cell. A sample cell with a long path length (5 – 10 cm) is needed because the gases show relatively weak absorbance.

UNIT – II

Raman Spectroscopy

FT Raman spectroscopy – degree of depolarization – structure determination using IR and Raman spectroscopy – Resonance Raman spectroscopy – Coherent anti-Stokes Raman spectroscopy – Inverse Raman and surface Enhanced Raman spectroscopy – principles, techniques and applications – nonlinear Raman spectroscopy

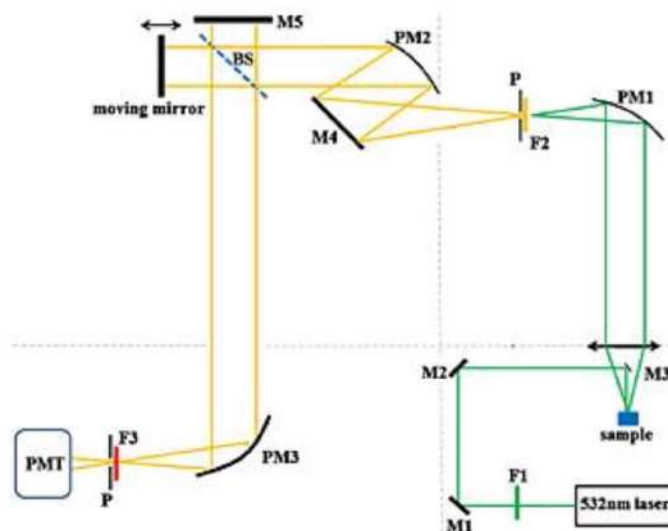
FT - RAMAN SPECTROSCOPY:

It is a spectroscopic technique used to observe vibrational, rotational, and other low-frequency modes in a system.^[1] It relies on inelastic scattering, or Raman scattering, of monochromatic light, usually from a laser in the visible, near infrared, or near ultraviolet range. The laser light interacts with molecular vibrations, phonons or other excitations in the system, resulting in the energy of the laser photons being shifted up or down. The shift in energy gives information about the vibrational modes in the system. Infrared spectroscopy yields similar, but complementary, information.

Typically, a sample is illuminated with a laser beam. Electromagnetic radiation from the illuminated spot is collected with a lens and sent through a monochromator. Elastic scattered radiation at the wavelength corresponding to the laser line (Rayleigh scattering) is filtered out, while the rest of the collected light is dispersed onto a detector by either a notch filter or a band pass filter.

Hence the three types of vibrational spectroscopy are complementary, all giving in theory the same frequency for a given vibrational transition, but the

relative intensities giving different information due to the types of interaction between the molecule and the electromagnetic radiation for infrared and Raman spectroscopy and with the neutron beam for IINS.



APPLICATION:

Raman spectroscopy is commonly used in chemistry, since vibrational information is specific to the chemical bonds and symmetry of molecules. Therefore, it provides a fingerprint by which the molecule can be identified. For instance, the vibrational frequencies of SiO , Si_2O_2 , and Si_3O_3 were identified and assigned on the basis of normal coordinate analyses using infrared and Raman spectra. The fingerprint region of organic molecules is in the (wavenumber) range $500\text{--}2000\text{ cm}^{-1}$. Another way that the technique is used is to study changes in chemical bonding, as when a substrate is added to an enzyme.

Raman gas analyzers have many practical applications. For instance, they are used in medicine for real-time monitoring of anesthetic and respiratory gas mixtures during surgery.

In solid state chemistry and the bio-pharmaceutical industry, Raman spectroscopy can be used to not only identify (ID) active pharmaceutical ingredients (APIs), but in the case of multiple polymorphic forms, it can also be used to identify the polymorphic form of the API. For example there are 4 different polymorphic forms of the API (aztreonam) in Cayston, a drug marketed by Gilead Sciences for cystic fibrosis.

Both infrared and Raman spectroscopy can be used to identify and characterize the API which is used in the formulation of Cayston. In bio-pharmaceutical formulations, one must use not only the correct molecule, but the correct polymorphic form, as different polymorphic forms have different physical properties, for example, solubility, melting point, and Raman/infrared spectra.

In solid-state physics, spontaneous Raman spectroscopy is used to, among other things, characterize materials, measure temperature, and find the crystallographic orientation of a sample. As with single molecules, a given solid material has characteristic phonon modes that can help an experimenter identify it. In addition, Raman spectroscopy can be used to observe other low frequency excitations of the solid, such as plasmons, magnons, and superconducting gap excitations. The spontaneous Raman signal gives information on the population of a given phonon mode in the ratio between the Stokes (downshifted) intensity and anti-Stokes (upshifted) intensity.

Raman scattering by an anisotropic crystal gives information on the crystal orientation. The polarization of the Raman scattered light with respect to the crystal and the polarization of the laser light can be used to find the orientation of the crystal, if the crystal structure (to be specific, its point group) is known.

Raman spectroscopy is the basis for Distributed Temperature Sensing (DTS) along optical fibers, which uses the Raman-shifted backscatter from laser pulses to determine the temperature along optical fibers.

DEGREE OF POLARIZATION:

Degree of polarization (DOP) is a quantity used to describe the portion of an electromagnetic wave which is polarized. A perfectly polarized wave has a DOP of 100%, whereas an unpolarized wave has a DOP of 0%. A wave which is partially polarized, and therefore can be represented by a superposition of a polarized and unpolarized component, will have a DOP somewhere in between 0 and 100%.

DOP is calculated as the fraction of the total power that is carried by the polarised component of the wave. DOP can be used to map the strain field in materials when considering the DOP of the photoluminescence. The polarization of the photoluminescence is related to the strain in a material by way of the given material's photoelasticity tensor.

DOP is also visualized using the Poincaré sphere representation of a polarized beam. In this representation, DOP is equal to the length of the vector measured from the center of the sphere.

TYPES:

(I) LINEAR POLARIZATION:

In electrodynamics, linear polarization or plane polarization of electromagnetic radiation is a confinement of the electric field vector or magnetic field vector to a given plane along the direction of propagation. See polarization for more information. The orientation of a linearly polarized electromagnetic wave is defined by the direction of the electric field vector.^[1] For example, if the electric field vector is vertical (alternately up and down as the wave travels) the radiation is said to be vertically polarized.

(II) CIRCULAR POLARIZATION:

In electrodynamics, circular polarization of an electromagnetic wave is a polarization in which the electric field of the passing wave does not change strength but only changes direction in a rotary manner.

In electrodynamics the strength and direction of an electric field is defined by what is called an electric field vector. In the case of a circularly polarized wave, as seen in the accompanying animation, the tip of the electric field vector, at a given point in space, describes a circle as time progresses. If the wave is frozen in time, the electric field vector of the wave describes a helix along the direction of propagation. Circular polarization is a limiting case of the more general condition of elliptical polarization. The other special case is the easier-to-understand linear polarization. The phenomenon of polarization arises as a consequence of the fact that light behaves as a two-dimensional transverse wave.

(III) ELLIPTICAL POLARIZATION:

In electrodynamics, elliptical polarization is the polarization of electromagnetic radiation such that the tip of the electric field vector describes an ellipse in any fixed plane intersecting, and normal to, the direction of propagation. An elliptically polarized wave may be resolved into two linearly polarized waves in phase quadrature, with their polarization planes at right angles to each other. Since the electric field can rotate clockwise or counterclockwise as it propagates, elliptically polarized waves exhibit chirality. Other forms of polarization, such as circular and linear polarization, can be considered to be special cases of elliptical polarization.

STRUCTURE DETERMINATION USING IR AND RAMAN SPECTROSCOPY:

So far, the emphasis has been on identification of the observed signals in the spectra and their correlation with the amino acid protons giving rise to the signals. Afterwards, one has to extract the data which are relevant for the structure. Of special importance in this respect are proton-proton distances, which can be estimated from the signal intensities in the 2D NOESY, 3D ¹⁵N-NOESY-HSQC and 3D ¹³C-NOESY-HSQC spectra .

Signal intensity depends on the distance r between two nuclei i and j , according to:

$$\text{NOE}_{ij} \sim 1/r_{ij}^6$$

Distances are derived from the spectra after calibration against NOE signals for known distances (such as distances in elements of secondary structure) and grouped into a few classes. An upper and a lower bound of distance is assigned to

each class. The lower bound is often set to the sum of the van der Waals radii of the two protons.

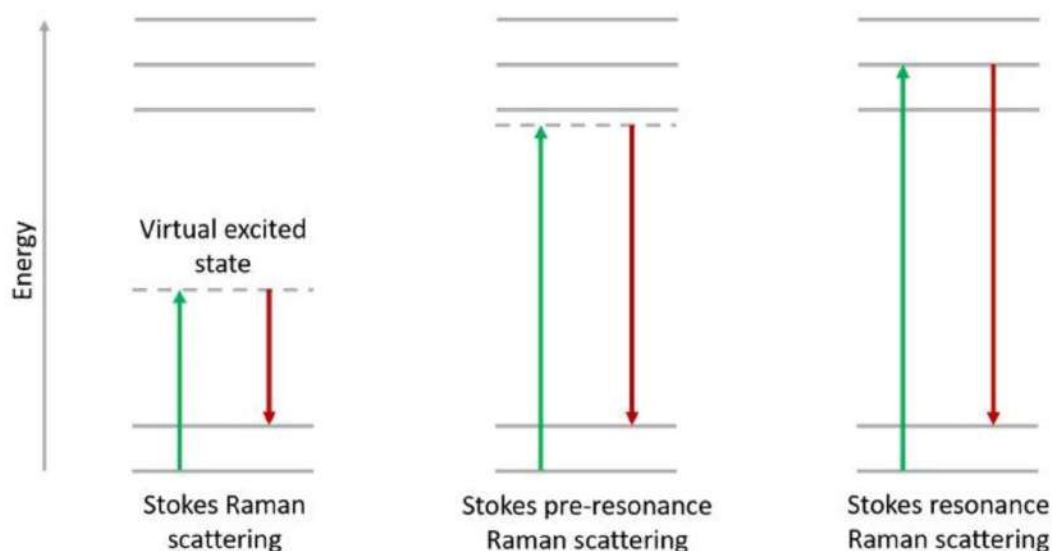
NOE class	distance [Å]	upper bound [Å]
very strong	2.3	2.5
strong	2.8	3.1
medium	3.1	3.4
weak	3.5	3.9
very weak	4.2	5.0

In this procedure, all non-sequential signals which are visible in the NOESY spectra have to be assigned, the number of which easily exceeds 1000 in a medium-sized protein (ca. 120 amino acids). It is distinguished between cross peaks of protons no more than five amino acids apart in the protein sequence (medium range NOE's) and those which are more than five amino acids apart (long range NOE's). The former are mainly indicative of the protein backbone conformation and are used for secondary structure determination, whereas the latter are an expression of the global structure of the protein and therefore contain the main information used for tertiary structure calculation.

RESONANCE RAMAN SPECTROSCOPY:

Resonance Raman (RR) spectroscopy is a type of vibrational Raman spectroscopy in which the incident laser frequency is close to an electronic transition of the molecule or crystal studied. The frequency coincidence (or

resonance) can lead to greatly enhanced intensity of the Raman spectra which facilitates the study of small samples.



If the electronic excitation is localized in a chromophore in one part of the molecule, then the vibrational transitions which are enhanced are primarily those which involve movement of atoms in the chromophore. For larger molecules, this selectivity helps to identify the vibrations observed.

COHERENT ANTI-STOKES RAMAN SPECTROSCOPY:

Coherent anti-Stokes Raman spectroscopy, also called Coherent anti-Stokes Raman scattering spectroscopy (CARS), is a form of spectroscopy used primarily in chemistry, physics and related fields. It is sensitive to the same vibrational signatures of molecules as seen in Raman spectroscopy, typically the nuclear vibrations of chemical bonds. Unlike Raman spectroscopy, CARS employs multiple photons to address the molecular vibrations, and produces a coherent signal.

As a result, CARS is orders of magnitude stronger than spontaneous Raman emission. CARS is a third-order nonlinear optical process involving three laser

beams: a pump beam of frequency ω_p , a Stokes beam of frequency ω_s and a probe beam at frequency ω_{pr} . These beams interact with the sample and generate a coherent optical signal at the anti-Stokes frequency ($\omega_{pr} + \omega_p - \omega_s$). The latter is resonantly enhanced when the frequency difference between the pump and the Stokes beams ($\omega_p - \omega_s$) coincides with the frequency of a Raman resonance, which is the basis of the technique's intrinsic vibrational contrast mechanism.

Coherent Stokes Raman spectroscopy (CSRS pronounced as "scissors") is closely related to Raman spectroscopy and lasing processes. It is very similar to CARS except it uses an anti-Stokes frequency stimulation beam and a Stokes frequency beam is observed (the opposite of CARS).

PRINCIPLE:

The CARS process can be physically explained by using either a classical oscillator model or by using a quantum mechanical model that incorporates the energy levels of the molecule. Classically, the Raman active vibrator is modeled as a (damped) harmonic oscillator with a characteristic frequency of ω_v . In CARS, this oscillator is not driven by a single optical wave, but by the difference frequency ($\omega_p - \omega_s$) between the pump and the Stokes beams instead.

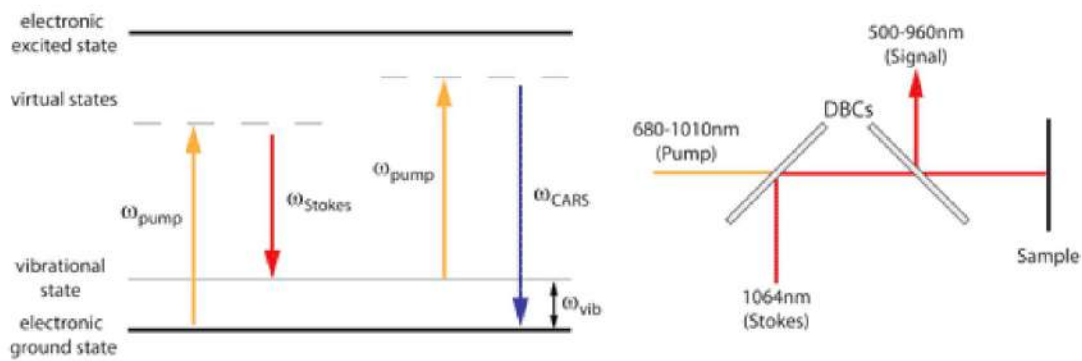
Working

This driving mechanism is similar to hearing the low combination tone when striking two different high tone piano keys: your ear is sensitive to the difference frequency of the high tones. Similarly, the Raman oscillator is susceptible to the difference frequency of two optical waves. When the difference frequency $\omega_p - \omega_s$ approaches ω_v , the oscillator is driven very efficiently. On a molecular level, this

implies that the electron cloud surrounding the chemical bond is vigorously oscillating with the frequency $\omega_p - \omega_s$. These electron motions alter the optical properties of the sample, i.e. there is a periodic modulation of the refractive index of the material. This periodic modulation can be probed by a third laser beam, the probe beam. When the probe beam is propagating through the periodically altered medium, it acquires the same modulation. Part of the probe, originally at ω_{pr} will now get modified to $\omega_{pr} + \omega_p - \omega_s$, which is the observed anti-Stokes emission. Under certain beam geometries, the anti-Stokes emission may diffract away from the probe beam, and can be detected in a separate direction.

While intuitive, this classical picture does not take into account the quantum mechanical energy levels of the molecule. Quantum mechanically, the CARS process can be understood as follows. Our molecule is initially in the ground state, the lowest energy state of the molecule. The pump beam excites the molecule to a virtual state.

A virtual state is not an eigenstate of the molecule and it can not be occupied but it does allow for transitions between otherwise uncoupled real states. If a Stokes beam is simultaneously present along with the pump, the virtual state can be used as an instantaneous gateway to address a vibrational eigenstate of the molecule. The joint action of the pump and the Stokes has effectively established a coupling between the ground state and the vibrationally excited state of the molecule. The molecule is now in two states at the same time: it resides in a coherent superposition of states.



This coherence between the states can be probed by the probe beam, which promotes the system to a virtual state. Again, the molecule cannot stay in the virtual state and will fall back instantaneously to the ground state under the emission of a photon at the anti-Stokes frequency. The molecule is no longer in a superposition, as it resides again in one state, the ground state.

In the quantum mechanical model, no energy is deposited in the molecule during the CARS process. Instead, the molecule acts like a medium for converting the frequencies of the three incoming waves into a CARS signal (a parametric process). There are, however, related coherent Raman processes that occur simultaneously which do deposit energy into the molecule.

INVERSE RAMAN SPECTROSCOPY:

The inverse Raman effect in optics (the branch of physics which deals with the properties and behavior of light) is a form of Raman scattering. It was first noted by W.J. Jones and B.P. Stoicheff.

If a material is simultaneously irradiated by intense monochromatic light of frequency ν_L (typically a laser beam) and light of a continuum of higher frequencies, among the possibilities for light scattering are scattering:

from the monochromatic beam at ν_L to the continuum at $\nu_L + \nu_M$ (anti-Stokes Raman scattering)

from the continuum at $\nu_L + \nu_M$ to the monochromatic beam at ν_L (Stokes Raman scattering)

where ν_M is a Raman frequency of the material. The strength of these two scatterings depends (among other things) on the energy levels of the material, their occupancy, and the intensity of the continuum. In some circumstances Stokes scattering can exceed anti-Stokes scattering; in these cases the continuum (on leaving the material) is observed to have an absorption line (a dip in intensity) at $\nu_L + \nu_M$. This phenomenon is referred to as the inverse Raman effect; the application of the phenomenon is referred to as inverse Raman spectroscopy, and a record of the continuum is referred to as an inverse Raman spectrum.

In the original description of the inverse Raman effect,^[1] the authors discuss both absorption from a continuum of higher frequencies and absorption from a continuum of lower frequencies. They note that absorption from a continuum of lower frequencies will not be observed if the Raman frequency of the material is vibrational in origin and if the material is in thermal equilibrium.

APPLICATIONS:

Raman spectroscopy is commonly used in chemistry, since vibrational information is specific to the chemical bonds and symmetry of molecules. Therefore, it provides a fingerprint by which the molecule can be identified.

Raman gas analyzers have many practical applications. For instance, they are used in medicine for real-time monitoring of anesthetic and respiratory gas mixtures during surgery.

In solid state chemistry and the bio-pharmaceutical industry, Raman spectroscopy can be used to not only identify (ID) active pharmaceutical ingredients (APIs), but in the case of multiple polymorphic forms, it can also be used to identify the polymorphic form of the API.

In solid-state physics, spontaneous Raman spectroscopy is used to, among other things, characterize materials, measure temperature, and find the crystallographic orientation of a sample. As with single molecules, a given solid material has characteristic phonon modes that can help an experimenter identify it.

In addition, Raman spectroscopy can be used to observe other low frequency excitations of the solid, such as plasmons, magnons, and superconducting gap excitations. The spontaneous Raman signal gives information on the population of a given phonon mode in the ratio between the Stokes (downshifted) intensity and anti-Stokes (upshifted) intensity.

Raman scattering by an anisotropic crystal gives information on the crystal orientation. The polarization of the Raman scattered light with respect to the crystal and the polarization of the laser light can be used to find the orientation of the crystal, if the crystal structure (to be specific, its point group) is known.

Raman spectroscopy is the basis for Distributed Temperature Sensing (DTS) along optical fibers, which uses the Raman-shifted backscatter from laser pulses to determine the temperature along optical fibers.

Raman active fibers, such as aramid and carbon, have vibrational modes that show a shift in Raman frequency with applied stress. Polypropylene fibers also exhibit similar shifts. The radial breathing mode is a commonly used technique to evaluate the diameter of carbon nanotubes. In nanotechnology, a Raman microscope can be used to analyze nanowires to better understand the composition of the structures.

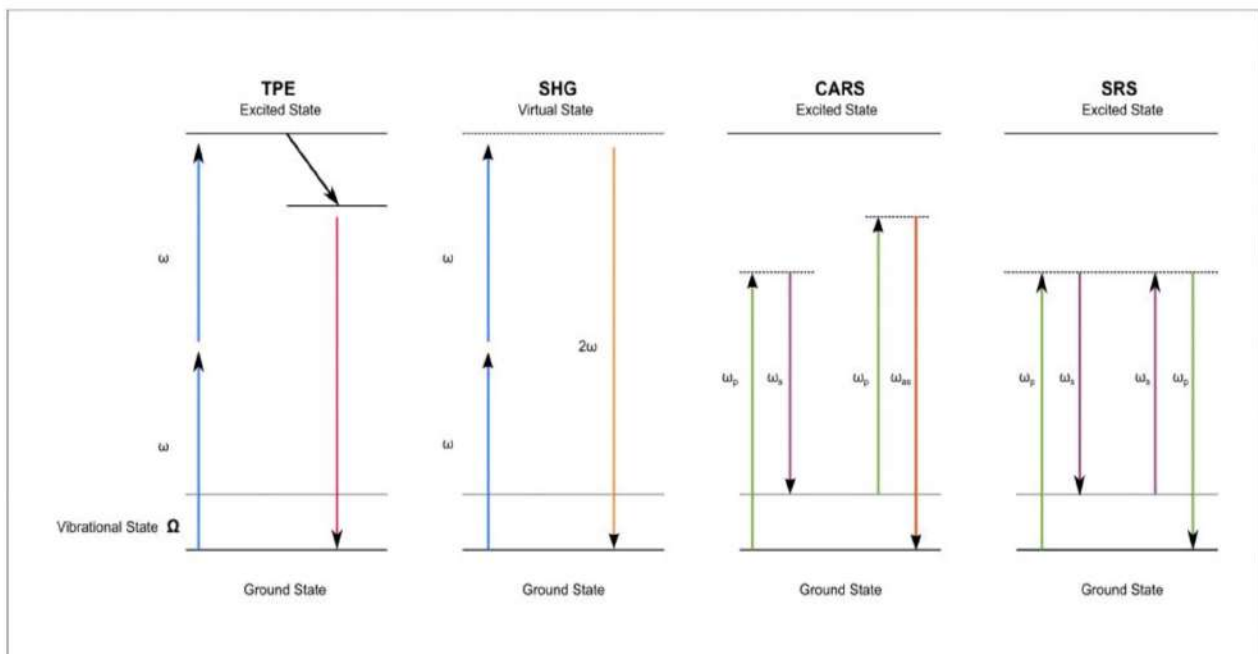
Spatially offset Raman spectroscopy (SORS), which is less sensitive to surface layers than conventional Raman, can be used to discover counterfeit drugs without opening their packaging, and for non-invasive monitoring of biological tissue. Raman spectroscopy can be used to investigate the chemical composition of historical documents such as the Book of Kells and contribute to knowledge of the social and economic conditions at the time the documents were produced. This is especially helpful because Raman spectroscopy offers a non-invasive way to determine the best course of preservation or conservation treatment for such materials.

NON-LINEAR SPECTROSCOPY:

There are many types of nonlinear optical techniques, and several depend on the spatial and temporal overlap of multiple optical pulses at different wavelengths on the target. Nonlinear spectroscopy results when a light field perturbs the optical properties of a molecule so that the subsequent light fields see changes in the molecular states. It is important that the different light fields

interact with the molecular states over time periods that are shorter than periods associated with dephasing and population relaxation so that the effects of the first interaction are not lost. By exciting a state with one light field and probing it at a later time, nonlinear experiments allow one to investigate how quantum states evolve in time and how different states are related to each other.

Within the different nonlinear optical spectroscopy techniques, raman spectroscopy (including Coherent anti-Stokes Raman Scattering (CARS) and Stimulated Raman Scattering (SRS)) are being developed for optical biopsy applications such as distinguishing cancer cells from normal cells. In order to be able to retrieve information for such applications, the sensitivity and speed of the techniques used is very important. Fig.1 shows the different energy level of techniques where sensitivity is high.



Energy Level Diagram of Different Nonlinear techniques including Two-Photon Excitation (TPE) and Second Harmonic Generation (SHG)

CARS uses two synchronized picosecond sources to stimulate a strong signal response at the Anti-Stokes frequency. This happens when the wavelengths of the two lasers are separated by a wavenumber matching the Raman transition of the sample. This technique is particularly suitable to detect lipids (fats) in microscopic cellular specimens. Ti:Sapphire (Ti:S) lasers and OPOs are used nowadays for CARS experiments as they match the application requirements. However, the drawback is their size and the complexity to maintain the two lasers synchronized.

Genia Photonics' synchronized programmable laser system uses its two laser outputs to generate CARS and SRS signals corresponding to the targeted wavenumbers. Since this compact laser system operates in the picosecond regime, the nonresonant background is eliminated allowing the acquisition of the information to be done very rapidly.

UNIT – III

Florescence and Phosphorescence Spectroscopy

Electronic Excitation of Diatomic Species – Vibrational Analysis of Band Systems of Diatomic Molecules – Deslandre's Table – Intensity Distribution – Franck Condon Principle – Rotational Structure of Electronic Bands – Resonance and Normal Fluorescence – Intensities of Transitions– phosphorescence Population of Triplet State and Intensity – Experimental Methods – Applications of Florescence and Phosphorescence.

ELECTRONIC EXCITATION OF DIATOMIC SPECIES:

The electronic-state configurations for molecules can be described by the primary quantum number n , the angular momentum quantum number Λ , the spin quantum number S , which remains a good quantum number, the quantum number Σ ($S, S-1, \dots, -S$), and the projection of the total angular momentum quantum number onto the molecular symmetry axis Ω , which can be derived as $\Omega = \Lambda + \Sigma$. The term symbol for the electronic states can be represented as

. Group theory makes great contributions to the prediction of the electronic selection rules for many molecules. An example is used to illustrate the possibility of electronic transitions via group theory.

1. The total spin cannot change, $\Delta S = 0$; the rule $\Delta \Sigma = 0$ holds for multiplets; If the spin-orbit coupling is not large, the electronic spin wavefunction can be separated from the electronic wavefunctions. Since the electron spin is a magnetic

effect, electronic dipole transitions will not alter the electron spin. As a result, the spin multiplicity should not change during the electronic dipole transition.

2. The total orbital angular momentum change should be $\Delta\Lambda=0, \pm 1$; For heteronuclear diatomic molecules with $C_{\infty v}$ symmetry, a $\Sigma^+ \leftrightarrow \Pi$ transition is allowed according to $\Delta\Lambda$ selection rule. In order to prove the allowance of this transition, the direct product of $\Sigma^+ \otimes \Pi$ yields Π irreducible representation from the direct product table. Based on the $C_{\infty v}$ character table below, the operator in the x and y direction have doubly degenerate Π symmetry. Therefore, the transition between $\Sigma^+ \leftrightarrow \Pi$ must be allowed since the multiplication of any irreducible representation with itself will provide the totally symmetric representation. The electronic transition moment integral can be nonzero. We can use the same kind of argument to illustrate that transition is forbidden.

3. Parity conditions are related to the symmetry of the molecular wavefunction reflecting against its symmetry axis. For homonuclear molecules, the $g \leftrightarrow u$ transition is allowed. For heteronuclear molecules, $+ \leftrightarrow +$ and $- \leftrightarrow -$ transitions apply;

The direct product of either $\Sigma^+ \otimes \Sigma^+$ or $\Sigma^- \otimes \Sigma^-$ yields the same irreducible representation Σ^+ based on the direct product table. The z component of the dipole operator has Σ^+ symmetry. The transition is allowed because the electronic transition moment integral can generate the totally symmetric irreducible representation Σ^+ . We can use the same method to prove that $\Sigma^+ \leftrightarrow \Sigma^-$ transitions are forbidden.

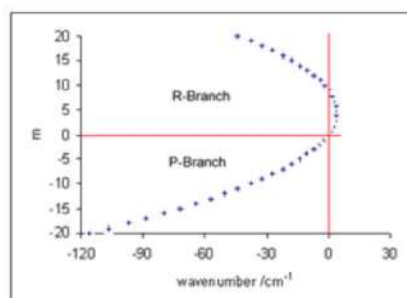
VIBRATIONAL ANALYSIS OF BAND SYSTEMS OF DIATOMIC MOLECULES:

The vibronic spectra of diatomic molecules in the gas phase also show rotational fine structure. Each line in a vibrational progression will show P- and R-branches. For some electronic transitions there will also be a Q-branch. The transition energies, expressed in wavenumbers, of the lines for a particular vibronic transition are given, in the rigid rotor approximation, that is, ignoring centrifugal distortion, by^[10]

$$G(J', J'') = \bar{\nu}_{v'-v''} + B' J'(J' + 1) - B'' J''(J'' + 1)$$

Here B are rotational constants and J are rotational quantum numbers. (For B also, a double prime indicates the ground state and a single prime an electronically excited state.) The values of the rotational constants may differ appreciably because the bond length in the electronic excited state may be quite different from the bond length in the ground state, because of the operation of the Franck-Condon principle.

The rotational constant is inversely proportional to the square of the bond length. Usually $B' < B''$ as is true when an electron is promoted from a bonding orbital to an antibonding orbital, causing bond lengthening. But this is not always the case; if an electron is promoted from a non-bonding or antibonding orbital to a bonding orbital, there will be bond-shortening and $B' > B''$.



Fortrat diagram created with $B'=0.8$, $B''=1$, showing displacement of rotational lines from the vibrational line position (at 0 cm^{-1}). Centrifugal distortion is ignored in this diagram.

The treatment of rotational fine structure of vibronic transitions is similar to the treatment of rotation-vibration transitions and differs principally in the fact that the ground and excited states correspond to two different electronic states as well as to two different vibrational levels. For the P-branch $J' = J'' - 1$, so that

$$\begin{aligned}\bar{\nu}_P &= \bar{\nu}_{v'-v''} + B'(J'' - 1)J'' - B''J''(J'' + 1) \\ &= \bar{\nu}_{v'-v''} - (B' + B'')J'' + (B' - B'')J''^2\end{aligned}$$

Similarly for the R-branch $J'' = J' - 1$, and

$$\begin{aligned}\bar{\nu}_R &= \bar{\nu}_{v'-v''} + B'J'(J' + 1) - B''J'(J' - 1) \\ &= \bar{\nu}_{v'-v''} + (B' + B'')J' + (B' - B'')J'^2\end{aligned}$$

Thus, the wavenumbers of transitions in both P- and R- branches are given, to a first approximation, by the single formula^{[10][11]}

$$\bar{\nu}_{P,R} = \bar{\nu}_{v',v''} + (B' + B'')m + (B' - B'')m^2, \quad m = \pm 1, \pm 2 \text{ etc.}$$

Here positive m values refer to the R-branch (with $m = +J'$) and negative values refer to the P-branch (with $m = -J''$). The wavenumbers of the lines in the P-branch, on the low wavenumber side of the *band origin* at $\bar{\nu}_{v',v''}$, increase with m . In the R-branch, for the usual case that $B' < B''$, as J increases the wavenumbers at first lie increasingly on the high wavenumber side of the band origin but then start to decrease, eventually lying on the low wavenumber side. The Fortrat

diagram illustrates this effect.^[note 2] In the rigid rotor approximation the line wavenumbers lie on a parabola which has a maximum at

$$x = -\frac{B' + B''}{2(B' - B'')}$$

The line of highest wavenumber in the R-branch is known as the *band head*. It occurs at the value of m which is equal to the integer part of x , or of $(x+1)$.

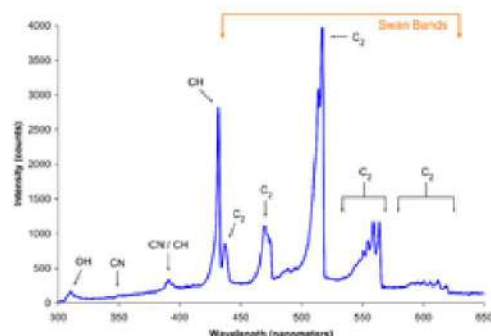
When a Q-branch is allowed for a particular electronic transition, the lines of the Q-branch correspond to the case $\Delta J=0$, $J=J''$ and wavenumbers are given by^[12]

$$\bar{\nu}_Q = \bar{\nu}_{v',v''} + (B' - B'')J(J + 1) \quad J = 1, 2 \text{ etc.}$$

The Q-branch then consists of a series of lines with increasing separation between adjacent lines as J increases. When $B' < B''$ the Q-branch lies to lower wavenumbers relative to the vibrational line.

The phenomenon of predissociation occurs when an electronic transition results in dissociation of the molecule at an excitation energy less than the normal dissociation limit of the upper state. This can occur when the potential energy curve of the upper state crosses the curve for a repulsive state, so that the two states have equal energy at some internuclear distance. This allows the possibility of a radiationless transition to the repulsive state whose energy levels form a continuum, so that there is blurring of the particular vibrational band in the vibrational progression.

APPLICATIONS:



Spectrum of the blue flame from a butane torch showing excited molecular radical band emission and Swan bands due to C_2 . The analysis of vibronic spectra of diatomic molecules provides information concerning both the ground electronic state and the excited electronic state. Data for the ground state can also be obtained by vibrational or pure rotational spectroscopy, but data for the excited state can only be obtained from the analysis of vibronic spectra.

For example, the bond length in the excited state may be derived from the value of the rotational constant B' . In addition to stable diatomic molecules, vibronic spectroscopy has been used to study unstable species, including CH, NH, hydroxyl radical, OH, and cyano radical, CN.^[14] The Swan bands in hydrocarbon flame spectra are a progression in the C-C stretching vibration of the dicarbon radical, C_2 for the $d^3\Pi_u \Leftrightarrow a^3\Pi_g$ electronic transition.^[15] Vibronic bands for 9 other electronic transitions of C_2 have been observed in the infrared and ultraviolet regions.

DESLANDRE'S TABLE:

In electronic spectroscopy, constructing a Deslandres table is a useful method to assign vibronic transitions. In such a table, the frequencies of the lines seen in an electronic spectrum of a molecule are collected so that the differences in energy between adjacent columns or rows are all the same (within experimental error). Every line seen in the spectrum corresponds to a transition from the lower-lying electronic energy state to an excited electronic state (molecular electronic transition): associated with this, there are corresponding transitions between the vibrational levels of the two states, that give rise to many closely spaced lines. The intensity of the lines is governed by the Franck–Condon principle.

trans-isomer of methacrolein (cm^{-1})

ν'	ν''					
	0	1	2	3	4	5
0	38*	34	31	27	22	
1	45	40				26
2			42	39		
3				46	41	

The numbers of absorption bands in Deslandres Tables 3 and 4 correspond to their numbers in Table 2.

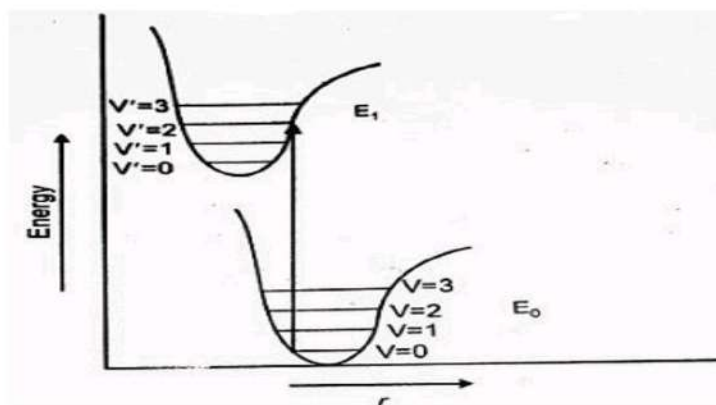
When a Deslandres table is filled correctly, the columns represent the vibrational energy levels of the lower electronic state (ν'), while the rows represent those for the upper electronic state (ν). Clearly, the difference in energy between two successive rows (columns) must remain constant for any column (row) in the table because this represents the energy difference of two given vibrational levels within the same electronic state.

Thus, by completing a Deslandres table it is easy to assign the correct vibrational quantum numbers ν'' and ν' for the transition, allowing important molecular properties to be calculated, such as the dissociation energy.

FRANCK CONDON PRINCIPLE:

Franck-Condon principle was proposed by German physicist James Franck (1882-1964) and U.S. physicist Edward U. Condon (1902-1974) in 1926. This principle states that when an electronic transition takes place, the time scale of this transition is so fast compared to nucleus motion that we can consider the nucleus to be static, and the vibrational transition from one vibrational state to another state is more likely to happen if these states have a large overlap. It successfully explains the reason why certain peaks in a spectrum are strong while others are weak (or even not observed) in absorption spectroscopy.

The second integral in the above equation is the vibrational overlap integral between one eigenstate and another eigenstate. In addition, the square of this integral is called the Franck-Condon factor. It governs the vibrational transition contribution to the transition probability and shows that in order to have a large vibrational contribution, the vibrational ground state and excited state must have a strong overlap.



The above figure shows the Franck-Condon principle energy diagram, since electronic transition time scale is small compared to nuclear motion, the vibrational transitions are favored when the vibrational transition have the smallest change of nuclear coordinate, which is a vertical transition in the figure above. The electronic eigenstates favors the vibrational transition $v'=0$ in the ground electronic state to $v''=2$ in the excited electronic state, while peak intensity of $v'=0$ to $v''=0$ transition is expected to be low because the overlap between the $v'=0$ wave function and $v''=0$ wave function is very low.

ROTATIONAL STRUCTURE OF ELECTRONIC BANDS:

The rotational structure of several violet absorption bands of ClO_2 has been studied. The bands considered correspond to the vibration transitions $(\nu_1' 0 0) \leftarrow (0 0 0)$ where $\nu_1' = 1, 2, 3, 4,$ and 5 . The most prominent identifiable feature of the rotational structure is a doublet qQ branch resolved in the tail of each band. For $\nu_1' = 1, 2,$ and 3 , the rotational wave numbers of these branches are given by This fits the spectrum in the observed range of quantum numbers, $K = 11$ to 20 and $L = K$ to $K+8$. The first two terms are associated with that prolate symmetrical top which comes closest to the actual ClO_2 molecule.

Hence, neglecting the effect of asymmetry on the spectrum, and The last term is associated with spin doubling. The coupling is shown to be close to Hund's "case b ." The linear terms in L and K may be a consequence of the doubling. The term in $\nu_1' K$ describes an outstanding feature of the spectrum but is not interpreted. The bands are shown to be of the parallel type. A few qP and qR branches have also been identified and $\Delta_1 F$ values have been found. Assuming the

spectrum to be that of a prolate symmetrical top, the resulting values of $2B$ for the vibrationless states are $2B'' = 0.612 \text{ cm}^{-1}$ and $2B' = 0.550 \text{ cm}^{-1}$.

The value of $2B''$ with the Cl-O distance $s'' = 1.53\text{A}$ from electron diffraction is sufficient to determine the lower electronic state. The upper state is then determined from the values of $2\Delta B$ and $2(\Delta A - \Delta B)$ for the vibrationless states. The resulting model of both states is designated as model (2). Error in this model, because of the fact that the effect of asymmetry was neglected, is found to be small. Asymmetry correction made on model (2) leads to the following model: The rotational isotope effect is observed and explained but gives no additional information about the molecular model.

RESONANCE AND NORMAL FLUORESCENCE:

The fluorescence of benzene vapor has been studied at pressures varying from 25 to 0.01 mm mercury using, as a monochromatic excitation source, the 2536A mercury line. At the lowest investigated pressures the emission spectrum consists of several narrow line groups. Their spacing shows that emission occurs in transitions from a definite vibrational level of the excited state to various vibrational levels of the normal state.

The following vibrational frequencies of the normal benzene molecule have been identified: 160, 793 (uncertain), 988, 1200, 1354, 1663 and 3139 cm^{-1} . The fine structure of the line groups has not been fully resolved. They appear to consist each of two strong lines with several weaker ones grouped around them. The ordinary, high pressure, fluorescence of benzene vapor is interpreted as being due to transitions from the lowest vibrational level of the excited state (or states).

This level is reached by molecules as the result of inelastic collisions upon excitation. An apparently continuous emission present at the long wave-length end of the fluorescence spectrum at higher vapor pressures is attributed to two causes, decreased intensity of bands heads owing to an increased moment of inertia of the molecule in higher vibrational levels of the normal state, and a crowding of vibrational levels when the total vibrational energy is large. This conclusion is supported by observations of the fluorescence of toluene, which appears to be almost wholly continuous.

FRET is a distance-dependent excited state interaction in which emission of one fluorophore is coupled to the excitation of another. It occurs primarily because the acceptor dipole interacts or resonates with the donor dipole. The use of FRET is to obtain structural maps of complex biological structures, primarily proteins and other macromolecular assemblies such as ribosomes and nucleosomes.

Measurements of energy transfer can provide intra- or intermolecular **distance** data for proteins and their ligands in the range 10-100 Angstrom. Also, FRET can detect **change in distance** (1-2 Angstrom) between loci in proteins, hence it is a sensitive measure of conformational change.

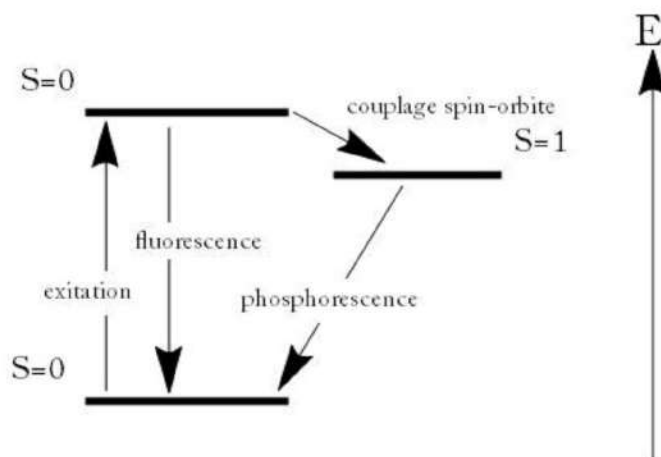
The distance between two residues in a protein can be determined from measurements of quantum yield or lifetime, if one residue has a fluorescence energy donor, and the other an energy acceptor. The efficiency of energy transfer measures the degree of overlap between the donor emission spectrum and acceptor absorption spectrum. This allows for determination of proximity and relative orientation of the fluorophores. The distance between the two is inversely proportional to the sixth power.

PHOSPHORESCENCE POPULATION OF TRIPLET STATE AND INTENSITY:

Fluorescence is the emission of light by a substance that has absorbed light or other electromagnetic radiation. It is a form of photoluminescence. In most cases, the emitted light has a longer wavelength, and therefore lower energy, than the absorbed radiation. However, when the absorbed electromagnetic radiation is intense, it is possible for one electron to absorb two photons; this two-photon absorption can lead to emission of radiation having a shorter wavelength than the absorbed radiation. The emitted radiation may also be of the same wavelength as the absorbed radiation, termed "resonance fluorescence".

Fluorescence occurs when an orbital electron of a molecule or atom relaxes to its ground state by emitting a photon of light after being excited to a higher quantum state by some type of energy. The most striking examples of fluorescence occur when the absorbed radiation is in the ultraviolet region of the spectrum, and thus invisible to the human eye, and the emitted light is in the visible region

Phosphorescence is a specific type of photoluminescence related to fluorescence. Unlike fluorescence, a phosphorescent material does not immediately re-emit the radiation it absorbs. Excitation of electrons to a higher state is accompanied with the change of a spin state. Once in a different spin state, electrons cannot relax into the ground state quickly because the re-emission involves quantum mechanically forbidden energy state transitions. As these transitions occur very slowly in certain materials, absorbed radiation may be re-emitted at a lower intensity for up to several hours after the original excitation.



Fluorescence and Phosphorescence

Energy scheme used to explain the difference between fluorescence and phosphorescence. Commonly seen examples of phosphorescent materials are the glow-in-the-dark toys, paint, and clock dials that glow for some time after being charged with a bright light such as in any normal reading or room light . Typically the glowing then slowly fades out within minutes (or up to a few hours) in a dark room.

EXPERIMENTAL METHODS:

A schematic of the full experimental apparatus is shown in Fig. S1. The output of a commercial regenerative amplifier (Coherent; Legend Elite USP; 800 nm, 40 fs, 0.9 mJ, 1 kHz) was used to pump a homebuilt mid-IR optical parametric amplifier (OPA) and visible noncollinear optical parametric amplifier (NOPA). The output of the NOPA (515 nm, 30 nm FWHM) was subsequently compressed to 20 fs with an AOPDF pulse shaper (Dazzler, Fastlite) (21) and characterized by self-referenced interferometry using cross-polarized wave generation (Wizzler, Fastlite) (40).

These devices were linked in a way that enabled an iterative feedback to correct for higher-order dispersion. The AOPDF pulse shaper was subsequently used to generate a pair of phase-locked pump pulses with precise control over the relative time delay between \mathbf{k}_1 and \mathbf{k}_2 , t_1 , and relative carrier-envelope phase, ϕ_{12} . These pulses were delayed on a delay stage and focused into the sample with an $f = 25$ cm, 90° off-axis parabolic silver mirror. At the sample position, the total power of the visible pump pulses, $\mathbf{k}_1 + \mathbf{k}_2$, was 270 nJ with a 350- μm spot size. The output of the mid-IR OPA was split into probe and reference pulses with a $\sim 50:50$ ZnSe beam splitter, and both focused into the sample with an $f = 15$ cm, 90° off-axis parabolic gold mirror.

Only the probe mid-IR probe pulse was overlapped with the visible pump. At the sample position, the power of the mid-IR pulses were measured to be ~ 100 nJ (~ 6 μm , 250- μm spot size) and the mid-IR pulse duration was measured to be ~ 90 fs via interferometric autocorrelation. Both probe and reference IR pulses were then collimated and focused into a spectrometer and frequency dispersed onto two 64-element HgCdTe arrays (Infrared Systems Development). The mid-IR reference signal was used to normalize the probe signal laser intensities, compensating for the instability and noise intrinsic to ultrafast mid-IR laser pulse generation and detection. The relative polarization of the visible pump and mid-IR probe pulse was set to magic angle (54.7°).

For each waiting time, t_2 , a 2D-EV surface was recorded by incrementing the relative phase of the pump \mathbf{k}_1 and \mathbf{k}_2 pulses for fixed t_1 time delays. We used a $3 \times 1 \times 1$ phase cycling routine and rotated the frame to 1,000 nm. The coherence time delay, t_1 , was incremented in 0.89-fs time steps between 0 and 80 fs and

therefore about double the sampling rate to satisfy the Nyquist–Shannon sampling theorem (at 1,000 nm, half the Nyquist frequency is 1.66 fs). Each data point that comprised a 2D-EV surface was acquired for 100 laser shots, and each surface was averaged three times. The 2D-EV spectra were collected for the values of t_2 between -275 and 600 fs in 25-fs steps, 700 fs and 5 ps in 100-fs steps, and 6 and 20 ps in 1-ps steps.

Separate pump-probe data were acquired using the same apparatus and conditions as detailed above, except the Dazzler was used to chop the pump pulses. The pump-probe data were recorded as $\Delta T/T$ and averaged for five scans.

DFT CALCULATIONS:

DFT calculations were performed in Gaussian 09 (41) using the ω B97-xD exchange-correlation functional, a 6-311+G* basis set and a polarized solvent continuum model with appropriate dielectric constant for the DMSO solvent.

SAMPLE:

DCM laser dye (Sigma-Aldrich) was dissolved in DMSO- d_6 to make a solution with an optical density of 0.4 at the maximum visible laser intensity (515 nm) in a flow cell with a 250- μ m path length (Fig. S2). The optical density of the ground-state IR transitions were \sim 0.02 (Fig. S3). The sample was prepared just before the start of experiments and continuously flowed throughout the measurement. All measurements were performed at 21 °C.

DATA ANALYSIS:

A Savitzky–Golay filter was applied to the data as to remove sharp water absorptions from the signal. Careful consideration was taken in this process such that the line widths in 2D-EV were unaffected by this filter and the apodization and zero padding.

APPLICATIONS OF FLORESCENCE AND PHOSPHORESCENCE:

The common fluorescent lamp relies on fluorescence. Inside the glass tube is a partial vacuum and a small amount of mercury. An electric discharge in the tube causes the mercury atoms to emit ultraviolet light. The tube is lined with a coating of a fluorescent material, called the *phosphor*, which absorbs the ultraviolet and re-emits visible light. Fluorescent lighting is more energy-efficient than incandescent lighting elements.

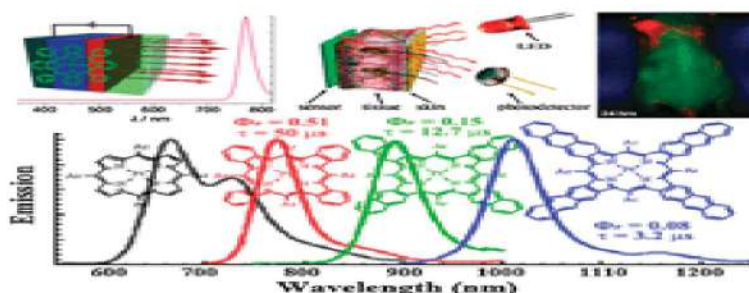
However, the uneven spectrum of traditional fluorescent lamps may cause certain colors to appear different than when illuminated by incandescent light or daylight. The mercury vapor emission spectrum is dominated by a short-wave UV line at 254 nm (which provides most of the energy to the phosphors), accompanied by visible light emission at 436 nm (blue), 546 nm (green) and 579 nm (yellow-orange). These three lines can be observed superimposed on the white continuum using a hand spectroscope, for light emitted by the usual white fluorescent tubes.

These Fluorescent lights were first available to the public at the 1939 New York World's Fair. Improvements since then have largely been better phosphors, longer life, and more consistent internal discharge, and easier-to-use shapes (such as compact fluorescent lamps). Some high-intensity discharge (HID) lamps couple

their even-greater electrical efficiency with phosphor enhancement for better color rendition.

White light-emitting diodes (LEDs) became available in the mid-1990s as LED lamps, in which blue light emitted from the semiconductor strikes phosphors deposited on the tiny chip. The combination of the blue light that continues through the phosphor and the green to red fluorescence from the phosphors produces a net emission of white light. Glow sticks sometimes utilize fluorescent materials to absorb light from the chemiluminescent reaction and emit light of a different color.

Moreover, NIR phosphorescence holds promise for *in vivo* imaging, because cells and tissues exhibit little absorption and auto-fluorescence in this spectral region. This review describes the overall progress made in the past ten years on NIR phosphorescent transition-metal complexes including Cu(I), Cu(II), Cr(III), Re(I), Re(III), Ru(II), Os(II), Ir(III), Pt(II), Pd(II), Au(I), and Au(III) complexes, with a primary focus on material design complemented with a selection of optical, electronic, sensory, and biologic applications. A critical comparison of various NIR phosphorescent materials reported in the literature and a blueprint for future development in this field are also provided.



UNIT – IV

NMR and NQR Spectroscopy

NMR Spectroscopy: Quantum Mechanical and Classical Description – Bloch Equation – Relaxation Process – Experimental Technique – Principle and Working of High Resolution NMR Spectrometer – Chemical Shift.

NQR Spectroscopy: Fundamental Requirements – General Principle – Experimental Detection of NQR Frequencies – Interpretation and Chemical Explanation of NQR Spectroscopy.

NMR- SPECTROSCOPY:

Nuclear magnetic resonance (NMR) is a physical phenomenon in which nuclei in a magnetic field absorb and re-emit electromagnetic radiation. This energy is at a specific resonance frequency which depends on the strength of the magnetic field and the magnetic properties of the isotope of the atoms; in practical applications, the frequency is similar to VHF and UHF television broadcasts (60–1000 MHz).

NMR allows the observation of specific quantum mechanical magnetic properties of the atomic nucleus. Many scientific techniques exploit NMR phenomena to study molecular physics, crystals, and non-crystalline materials through NMR spectroscopy. NMR is also routinely used in advanced medical imaging techniques, such as in magnetic resonance imaging (MRI).

A key feature of NMR is that the resonance frequency of a particular substance is directly proportional to the strength of the applied magnetic field. It is this feature that is exploited in imaging techniques; if a sample is placed in a non-

uniform magnetic field then the resonance frequencies of the sample's nuclei depend on where in the field they are located.

Since the resolution of the imaging technique depends on the magnitude of magnetic field gradient, many efforts are made to develop increased field strength, often using superconductors. The effectiveness of NMR can also be improved using hyperpolarization, and/or using two-dimensional, three-dimensional and higher-dimensional multi-frequency techniques.

The principle of NMR usually involves two sequential steps:

The alignment (polarization) of the magnetic nuclear spins in an applied, constant magnetic field \mathbf{H}_0 . The perturbation of this alignment of the nuclear spins by employing an electro-magnetic, usually radio frequency (RF) pulse. The required perturbing frequency is dependent upon the static magnetic field (\mathbf{H}_0) and the nuclei of observation.

The two fields are usually chosen to be perpendicular to each other as this maximizes the NMR signal strength. The resulting response by the total magnetization (\mathbf{M}) of the nuclear spins is the phenomenon that is exploited in NMR spectroscopy and magnetic resonance imaging. Both use intense applied magnetic fields (\mathbf{H}_0) in order to achieve dispersion and very high stability to deliver spectral resolution, the details of which are described by chemical shifts, the Zeeman effect, and Knight shifts (in metals).

NMR phenomena are also utilized in low-field NMR, NMR spectroscopy and MRI in the Earth's magnetic field (referred to as Earth's field NMR), and in several types of magnetometers.

The Quantum Mechanical Description of NMR:

The quantum mechanical description of atomic nuclei, as described by Dirac in 1930, predicted the property of spin angular momentum. In fact the property of electron spin was observed six years earlier by Stern and Gerlach, who passed a beam of neutral atoms through a non-uniform magnetic field, and observed the effect of half-integral angular momentum, that could not be explained by the previously accepted Bohr model.

This spin angular momentum is characterised by the spin quantum number I , such that the total spin angular momentum is Ih . The value of I is an intrinsic property of the nucleus, examples of which are given in Table.

Nucleus	Spin Quantum
	Number
	I
^1H	1/2
^2H	1
^{12}C	0
^{13}C	1/2
^{19}F	1/2
^{31}P	1/2

Spin quantum numbers for some atomic nuclei

To exhibit the property of magnetic resonance the nucleus must have a non-zero value of I . As far as medical applications are concerned, the proton (^1H) is the nucleus of most interest, because of its high natural abundance. However, other nuclei have been studied, most noticeably ^{13}C whose low natural abundance relative to ^{12}C makes it suitable for tracer studies.

The magnitude of the spin angular momentum is given by $|\mathbf{P}| = \hbar\sqrt{I(I+1)}$

but since \mathbf{P} is a vector, its orientation must be taken into account. In a magnetic field, applied along the z axis, the possible values of the z -components of the angular momentum are given by

$$P_z = \hbar m_I$$

Where

$$m_I = I, (I-1), (I-2), \dots, -I.$$

So for the proton, with spin $1/2$, there are two possible values for P_z , that is $\pm \frac{1}{2}\hbar$. The eigenfunction describing the spin state of the proton nucleus can be written as $|+\frac{1}{2}\rangle$ or $|-\frac{1}{2}\rangle$, and since in quantum mechanics every physical observable has an associated operator, we can write an eigenvalue equation to describe the observation of the spin state as

$$I_z |m_I\rangle = m_I |m_I\rangle$$

where I_z is the operator describing measurement of the angular momentum along the z axis. There are similar operators for measuring the angular momentum along

the x and y axes, so we have a range of eigenvalue equations for a spin 1/2 system as follows:

$$\begin{aligned}
 I_x|+\frac{1}{2}\rangle &= +\frac{1}{2}|+\frac{1}{2}\rangle & I_x|-\frac{1}{2}\rangle &= -\frac{1}{2}|-\frac{1}{2}\rangle \\
 I_y|+\frac{1}{2}\rangle &= +\frac{1}{2}i|-\frac{1}{2}\rangle & I_y|-\frac{1}{2}\rangle &= +\frac{1}{2}i|+\frac{1}{2}\rangle \\
 I_z|+\frac{1}{2}\rangle &= +\frac{1}{2}|+\frac{1}{2}\rangle & I_z|-\frac{1}{2}\rangle &= -\frac{1}{2}|-\frac{1}{2}\rangle
 \end{aligned}$$

$$i = \sqrt{-1}$$

To measure the energy of the spin system it is necessary to construct a Hamiltonian operator. The form of the Hamiltonian can be derived from classical electromagnetism for the energy of a magnetic moment placed in a magnetic field.

Nuclei have a magnetic moment, \mathbf{m} , which is proportional to the angular momentum,

$$\mathbf{m} = \gamma \mathbf{P}$$

Nuclei with the constant of proportionality, γ , being called the magnetogyric ratio. The magnetogyric ratio is a property of the particular nucleus, and has a value of 2.675×10^8 rad/s/T for protons. When this magnetic moment is placed in a magnetic field, \mathbf{B} , it has energy

$$E = -\mathbf{m} \cdot \mathbf{B}$$

and so by combining equations 2.5 and 2.6 a Hamiltonian can be defined as

$$H = -\hbar \gamma \mathbf{B} \cdot \mathbf{I}$$

Since by definition the B field is applied parallel to the z-axis the Hamiltonian becomes

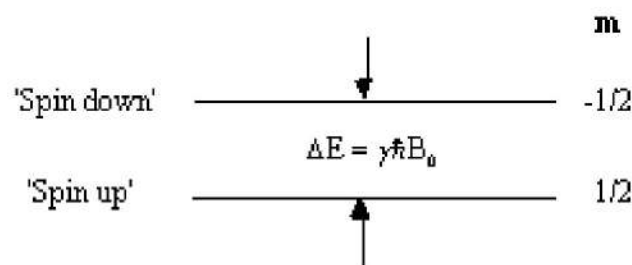
$$H = -\hbar \gamma B_z I_z$$

and is known as the Zeeman Hamiltonian. Now using the Schrödinger equation, the energy of the eigenstate is found.

$$\begin{aligned}
 H|m_I\rangle &= E|m_I\rangle \\
 &= -\hbar \gamma B_z I_z |m_I\rangle \\
 &= -\hbar \gamma B_z m_I |m_I\rangle \\
 \therefore E &= -\hbar \gamma B_z m_I.
 \end{aligned}$$

So for a proton with $m_I = \pm \frac{1}{2}$, a transition between the two states represents a change in energy

$$\Delta E = \hbar \gamma B_z$$



Energy level diagram for a proton under the Zeeman interaction.

This is called the Zeeman splitting, and is shown as an energy level diagram in Figure. These two states are given a variety of labels, but most commonly referred to as 'spin up', and 'spin down', with the spin-down state having a higher energy than the spin-up state. Transitions between the two states can be induced by absorption or emission of a photon of frequency ν_0 , such that

$$\begin{aligned}
 \Delta E &= \hbar \gamma B_z = h \nu \\
 \therefore \nu &= \frac{\gamma}{2\pi} B_z
 \end{aligned}$$

Expressing the frequency in angular terms gives the Larmor equation which underpins the whole of NMR

$$\omega = \gamma B_0$$

the characteristic frequency, ω , being the Larmor frequency. The magnetic field, labelled B_0 , is still assumed to be applied along the z axis, and is now subscripted with a '0' to distinguish it from the applied radio frequency field which will be introduced later.

This description of the quantum mechanical behaviour of an atomic nucleus leads to the way NMR is performed. Transitions between the two energy states, spin-up and spin-down, can occur by absorption or emission of electromagnetic radiation of frequency given by the Larmor equation. This frequency depends, for a given species of nuclei, purely on the applied magnetic field. It is the strength of the field experienced by the nucleus that enables structure to be determined in spectroscopy experiments, and position to be found in imaging experiments.

In a real system there is not just one nucleus in isolation, but many nuclei all of which could occupy a particular spin state. This means that the theory must be extended to consider an ensemble of spins.

To do this a single eigenstate Y , which is a linear combination of the possible spin states for a single nucleus is defined

$$|\Psi\rangle = \sum_{m_I} \alpha_{m_I} |m_I\rangle$$

When making a measurement on such a system, the expectation value of the operation on this superposition of states is

$$\langle \Psi | I_z | \Psi \rangle = \sum_{m_i} |a_{m_i}|^2 m_i$$

where the value $|a_{m_i}|^2$ represents the probability of finding a single nucleus in the state m_i . So for the case of a proton, with two spin states

$$|\Psi\rangle = a_{+\frac{1}{2}}|+\frac{1}{2}\rangle + a_{-\frac{1}{2}}|-\frac{1}{2}\rangle$$

The ratio of the populations of the two energy states from Boltzman statistics is

$$\begin{aligned} \frac{|a_{-\frac{1}{2}}|^2}{|a_{+\frac{1}{2}}|^2} &= \exp\left(\frac{-\Delta E}{k_B T}\right) \\ &= \exp\left(\frac{-\hbar \gamma \mathcal{B}_0}{k_B T}\right) \\ &\approx 1 - \frac{\hbar \gamma \mathcal{B}_0}{k_B T} \quad \text{provided } k_B T \gg \hbar \gamma \mathcal{B}_0. \end{aligned}$$

so the difference between the number of spins in the spin-up state and the spin-down state is

$$\begin{aligned} |a_{+\frac{1}{2}}|^2 - |a_{-\frac{1}{2}}|^2 &\approx |a_{+\frac{1}{2}}|^2 \cdot \frac{\hbar \gamma \mathcal{B}_0}{k_B T} \\ &\approx \frac{\hbar \gamma \mathcal{B}_0}{2k_B T} \end{aligned}$$

If we now assume that all the 'spin up' nuclei have a magnetic moment of $\frac{1}{2}\hbar \gamma$ and the 'spin down' nuclei have a magnetic moment of $-\frac{1}{2}\hbar \gamma$, then we can write the bulk magnetisation of the ensemble as

$$\mathbf{M} = N \left(\frac{\hbar \gamma}{2} \right) \left(\frac{\hbar \gamma E_0}{2k_B T} \right)$$

$$\approx N \left(\frac{\hbar \gamma}{2} \right)^2 \frac{E_0}{k_B T}$$

Where N is the number of spins in the ensemble. Being able to treat the behavior of all the spins in the system in terms of magnetization allows a transfer from a quantum mechanical to a classical description of NMR. The advantage of the classical description is that it gives a simpler picture of the NMR experiment.

BLOCH EQUATION:

In physics and chemistry, specifically in nuclear magnetic resonance (NMR), magnetic resonance imaging (MRI), and electron spin resonance (ESR), the **Bloch equations** are a set of macroscopic equations that are used to calculate the nuclear magnetization $\mathbf{M} = (M_x, M_y, M_z)$ as a function of time when relaxation times T_1 and T_2 are present. These are phenomenological equations that were introduced by Felix Bloch in 1946.^[1] Sometimes they are called the equations of motion of nuclear magnetization. They are analogous to the Maxwell-Bloch equations.

Bloch equations in laboratory (stationary) frame of reference

Let $\mathbf{M}(t) = (M_x(t), M_y(t), M_z(t))$ be the nuclear magnetization. Then the Bloch equations read:

$$\frac{dM_x(t)}{dt} = \gamma(\mathbf{M}(t) \times \mathbf{B}(t))_x - \frac{M_x(t)}{T_2}$$

$$\frac{dM_y(t)}{dt} = \gamma(\mathbf{M}(t) \times \mathbf{B}(t))_y - \frac{M_y(t)}{T_2}$$

$$\frac{dM_z(t)}{dt} = \gamma(\mathbf{M}(t) \times \mathbf{B}(t))_z - \frac{M_z(t) - M_0}{T_1}$$

Where γ is the gyromagnetic ratio and $\mathbf{B}(t) = (B_x(t), B_y(t), B_0 + \Delta B_z(t))$ is the magnetic field experienced by the nuclei. The z component of the magnetic field \mathbf{B} is sometimes composed of two terms:

One, B_0 , is constant in time,

The other one, $\Delta B_z(t)$, may be time dependent. It is present in magnetic resonance imaging and helps with the spatial decoding of the NMR signal.

$\mathbf{M}(t) \times \mathbf{B}(t)$ is the cross product of these two vectors. M_0 is the steady state nuclear magnetization (that is, for example, when $t \rightarrow \infty$); it is in the z direction.

RELAXATION PROCESS:

An understanding of relaxation processes is important for the proper measurement and interpretation of NMR spectra. There are three important considerations.

1. The very small energy difference between α and β states of a nuclear spin orientation in a magnetic field results in a very small excess population of nuclei in the ground vs the excited states (typically less than 1 out of about 10,000 molecules). For many nuclei relaxation (i.e., return from excited to ground state) is a very slow process, with half-lives on the order of 0.1 to 100 seconds for a spin $\frac{1}{2}$ nucleus (compare this with micro-, pico- and femtoseconds for relaxation of electronic and vibrational transitions). It is thus very easy to saturate an NMR transition (equalize populations of excited and ground state), with the resultant loss in signal quality, and failure to obtain correct peak areas.

2. NMR lines are extraordinarily sharp, and extraordinarily close together (in energetic terms) compared to higher energy spectroscopic methods. So much so that Heisenberg uncertainty broadening (which is a function of lifetime of a given energy state, and hence relaxation rates) is a dominant feature of many NMR spectra, and can limit our ability to measure and interpret spectra. When relaxation is very fast, NMR lines are broad, J -coupling may not be resolved or the signal may even be difficult or impossible to detect.

3. The success of many multipulse experiments, especially 2D and 3D spectra, depends crucially on proper consideration of relaxation times.

T_1 and T_2 Relaxation:

We distinguish two types of relaxation, *Spin-Lattice* (T_1 , also known as longitudinal relaxation, or relaxation in the z -direction) and *Spin-Spin* (T_2 , also known as transverse relaxation, or relaxation in the x - y plane). T_1 relaxation corresponds to the process of establishing (or re-establishing) the normal Gaussian population distribution of α and β spin states in the magnetic field.

T_2 is loss of phase coherence among nuclei. T_2 is less than or equal to T_1 ($R =$ relaxation rate, $R_2 = 1/T_2$, $R_2 \geq R_1$), since return of magnetization to the z -direction inherently causes loss of magnetization in the x - y plane. The line width of an NMR signal is determined by T_2 - short T_2 means broader lines ($\nu_{1/2} = 1/\pi T_2$, $\nu_{1/2} =$ width at half height). The maximum repetition rate during acquisition of an NMR signal is governed by T_1 - short T_1 means the magnetization recovers more rapidly, and a spectrum can be acquired in less time.

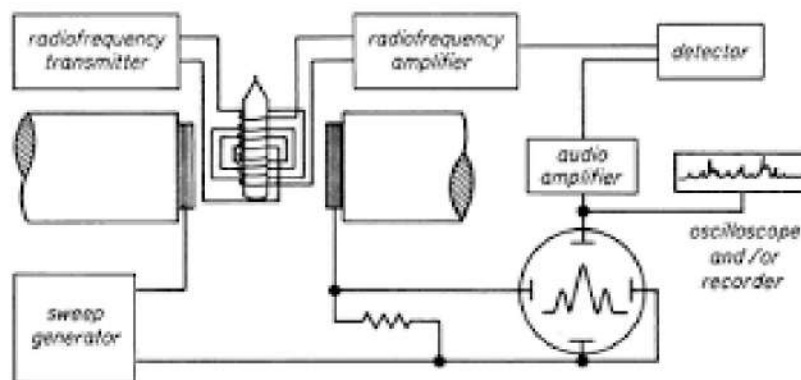
EXPERIMENTAL TECHNIQUES OF NMR SPECTROSCOPY:

When placed in a magnetic field, NMR active nuclei (such as ^1H or ^{13}C) absorb electromagnetic radiation at a frequency characteristic of the isotope.^[2] The resonant frequency, energy of the absorption, and the intensity of the signal are proportional to the strength of the magnetic field. For example, in a 21 Tesla magnetic field, protons resonate at 900 MHz. It is common to refer to a 21 T magnet as a 900 MHz magnet, although different nuclei resonate at a different frequency at this field strength in proportion to their nuclear magnetic moments.

ACQUISITION OF SPECTRA:

Upon excitation of the sample with radio frequency pulse, a nuclear magnetic resonance response - a free induction decay (FID) - is obtained. It is a very weak signal, and requires sensitive radio receivers to pick up. A Fourier transform is done to extract the frequency-domain spectrum from the raw time-domain FID. A spectrum from a single FID has a low signal-to-noise ratio, but fortunately it improves readily with averaging of repeated acquisitions. Good ^1H NMR spectra can be acquired with 16 repeats, which takes only minutes.

However, for heavier elements than hydrogen, the relaxation time is rather long, e.g. around 8 seconds for ^{13}C . Thus, acquisition of quantitative heavy-element spectra can be time-consuming, taking tens of minutes to hours. If the second excitation pulse is sent prematurely before the relaxation is complete, the average magnetization vector still points in a nonparallel direction, giving suboptimal absorption and emission of the pulse. In practice, the peak areas are then not proportional to the stoichiometry; only the presence, but not the amount of functional groups is possible to discern.



Nuclear Magnetic Resonance (NMR) spectroscopy, a physical phenomenon based upon the magnetic properties of certain atomic nuclei, has found a wide range of applications in life sciences over recent decades. The dramatic advances in NMR techniques have led to corresponding advances in the ability of NMR to study structure, dynamics and interactions of biological macromolecules in solution under close to physiological conditions. This volume focuses on the use of NMR to study proteins.

NMR can be used to determine detailed three-dimensional structures of proteins in solution. Furthermore, it provides information about conformational or chemical exchange, internal mobility and dynamics at timescales varying from picoseconds to seconds. It is the primary technique used to obtain information on intrinsically disordered (unfolded) proteins, since these proteins will not crystallize easily. NMR is also a very powerful method for the study of interactions of protein with other molecules, whether small molecules (including drugs), nuclear acids or other proteins.

This up-to-date volume covers NMR techniques and their application to proteins, with a focus on practical details. This book will provide a newcomer to NMR with the practical guidance in order to carry out successful experiments with proteins and to analyze the resulting spectra. Those who are familiar with the chemical applications of NMR will also find it useful in understanding the special requirements of protein NMR.

PRINCIPLE AND WORKING OF HIGH RESOLUTION NMR SPECTROMETER:

Nuclei with non-zero spins, when placed in a strong magnetic field precess at specific orientations with respect to the applied magnetic field. When appropriate energy is supplied in the form of radio frequency, these nuclei flip to a higher energy state. The energy absorbed during this transition is a function of nucleus type and its chemical environment in the molecule.

The excited nuclei are allowed to precess freely and come back to their equilibrium positions. During this process an electric signal is induced in a suitably placed RF coil. This signal which is monitored with respect to time is called free induction decay (FID). The FID, which is in time domain gives its equivalent frequency domain signal on Fourier transformation. A plot of the absorption frequency versus the intensity of the absorption constitutes the NMR spectrum.

APPLICATIONS:

Major application of NMR spectroscopy lies in the area of synthetic organic chemistry, inorganic chemistry, bio-organic chemistry, bio-inorganic chemistry, polymer chemistry and organometallic chemistry. One of the main advantages of

FT-NMR spectroscopy is that a number of FIDs can be accumulated and Fourier transformed, enhancing S/N ratio of the spectrum. This in turn facilitates the analysis of samples with low abundant nuclei and smaller gyro-magnetic ratios, e.g., ^{13}C , ^{29}Si , ^{15}N etc.

Another major advantage of pulse NMR is that by suitably programming, a variety of pulse sequences can be generated and applied to obtain diverse information like relaxation times, connectivity through bond and through space etc. Thus, by using FT-NMR it is not only possible to get the information about chemical shift and spin-spin coupling but also possible to deduce the conformational structural information of a particular molecule.

CHEMICAL SHIFT:

In nuclear magnetic resonance (NMR) spectroscopy, the **chemical shift** is the resonant frequency of a nucleus relative to a standard. Often the position and number of chemical shifts are diagnostic of the structure of a molecule.^{[1][2][3]} Chemical shifts are also used to describe signals in other forms of spectroscopy such as photoemission spectroscopy.

Some atomic nuclei possess a magnetic moment (nuclear spin), which gives rise to different energy levels and resonance frequencies in a magnetic field. The total magnetic field experienced by a nucleus includes local magnetic fields induced by currents of electrons in the molecular orbitals (note that electrons have a magnetic moment themselves).

The electron distribution of the same type of nucleus (e.g. ^1H , ^{13}C , ^{15}N) usually varies according to the local geometry (binding partners, bond lengths,

angles between bonds, ...), and with it the local magnetic field at each nucleus. This is reflected in the spin energy levels (and resonance frequencies).

The variations of nuclear magnetic resonance frequencies of the same kind of nucleus, due to variations in the electron distribution, are called the chemical shift. The size of the chemical shift is given with respect to a reference frequency or reference sample. Usually a molecule with a barely distorted electron distribution.

CHEMICAL SHIFT REFERENCING:

Chemical shift δ is usually expressed in parts per million (ppm) by frequency, because it is calculated from:

$\delta = \frac{\text{difference between a resonance frequency and that of a reference substance}}{\text{operating frequency of the spectrometer}}$

Since the numerator is usually in hertz, and the denominator in megahertz, delta is expressed in ppm.

The detected frequencies (in Hz) for ^1H , ^{13}C , and ^{29}Si nuclei are usually referenced against TMS (tetramethylsilane) or DSS, which is assigned the chemical shift of zero. Other standard materials are used for setting the chemical shift for other nuclei.

Thus, an NMR signal that absorbs at 300 Hz higher than does TMS at an applied frequency of 300 MHz has a chemical shift of:

$$\frac{300\text{Hz}}{300 \times 10^6\text{Hz}} = 1 \times 10^{-6} = 1\text{ppm}$$

Although the frequency depends on the applied field, the chemical shift is independent of it. On the other hand the resolution of NMR will increase with applied magnetic field.

CHEMICAL SHIFT AND MAGNETIC RESONANCE SPECTROSCOPY:

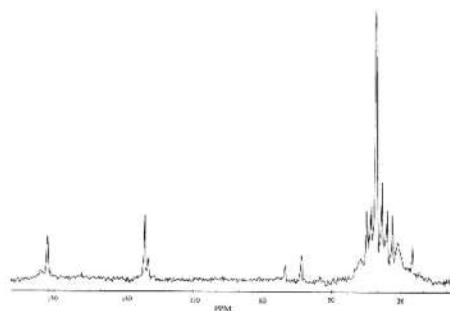
The electrons that surround each nucleus can act to slightly perturb the magnetic field at the spin site. This causes the Larmor precession frequency to be modified by the chemical environment of the spin. The effect of chemical shift is described by the equation

$$B = (1 - \sigma)B_0$$

Where σ is the shielding constant. This modifies the Larmor frequency such that

$$\omega = \gamma(1 - \sigma)B_0$$

And is detected upon Fourier transformation of the FID as a shift in frequency away from that expected if chemical shift played no part. For a sample containing spins with a number of different chemical shifts, the resulting spread of frequencies represents a chemical spectrum. An example of an NMR spectrum is shown in Figure



It is common to express the chemical shift of a peak in the spectrum in terms of the relative difference in frequency from some reference peak. The chemical shift in parts per million (p.p.m.) is therefore defined as

$$\delta = \frac{\nu - \nu_{\text{ref}}}{\nu_{\text{ref}}} \cdot 10^6 \text{ p.p.m.}$$

Where ν and ν_{ref} are the resonant frequencies of the spectral peak of interest and the reference component respectively. Chemical shifts in ^1H spectra are of the order of a few p.p.m.

Another spin effect that is useful in MRS is the scalar, or spin-spin coupling. This arises from interactions between the nuclear spins, mediated by the delocalised electrons. However this effect is not very important in imaging, since its magnitude is so small. There are a number of other features of spin behaviour which affect the NMR signal. Some of these will be described, where appropriate, in other chapters.

FUNDAMENTAL REQUIREMENTS OF NQR:

GENERAL PRINCIPLE OF NQR:

The physical principles of Nuclear Quadrupole Resonance (NQR hereafter) are quite similar to those of Nuclear Magnetic Resonance (NMR). Let us start with NMR, which also historically (first experimental demonstration in 1946) precede NQR and remains to the present day much better developed. The motive force behind NMR detection and spectroscopic methods, is the magnetic moment of the nuclei in a substance.

The protons in the nuclei of a substance have a positive electric charge. Because they spin, this gives rise to a magnetic moment, that is, the proton acts like a tiny bar magnet. Quantum mechanics dictates that when such nuclei are subject to an externally applied magnetic field, they must align themselves along it. The alignment allows only two possible orientations: one in the same direction as the applied magnetic field, and another opposite to it.

Due to thermal excitation of the nuclei, almost half of the nuclei's magnetic moments will be aligned anti-parallel, and slightly more nuclei will be aligned parallel to the magnetic field. When the magnetic field is switched off, the nuclei will return to their standard thermal distribution, releasing an energy whose spectrum is typical of the substance involved. By spectroscopic analysis one can readily verify the nature of the compound. A short video that shows this process, can be found on the quantum magnetism website.

NQR works pretty much the same way, but there are some striking differences. First of all, NQR works by applying an external electrical field, rather than a magnetic field. Electric fields are easier to generate, and a device to produce an electric field of a given strength is considerably more portable than its magnetic equivalent. The drawback, is that NQR only works when the substance contains an appreciable quadrupole moment.

The quantum physical basis for the arising of quadrupole moments in some substances, is due to their nuclei having a spin number greater than $1/2$. When this is the case, the charge density is no longer spherically symmetrical. Instead, the charge density is described by the so-called quadrupole tensor Q . Some 74% of NMR active nuclei have a spin greater than $1/2$, and as a consequence possess a

quadrupole moment. Most studied examples include Deuterium, Nitrogen 14, Chlorine 37, Copper 63, Zinc 67, or Iodine 127.

The quadrupole moment interacts with any electric field gradient. In particular, it interacts with the local electric field generated by the molecular structure of the compound containing the quadrupole moment -from which it gets its compound-specific NQR spectrum- and it interacts with any externally applied field. By applying an external RF field, we can align the spins and see them relax when we terminate the field.

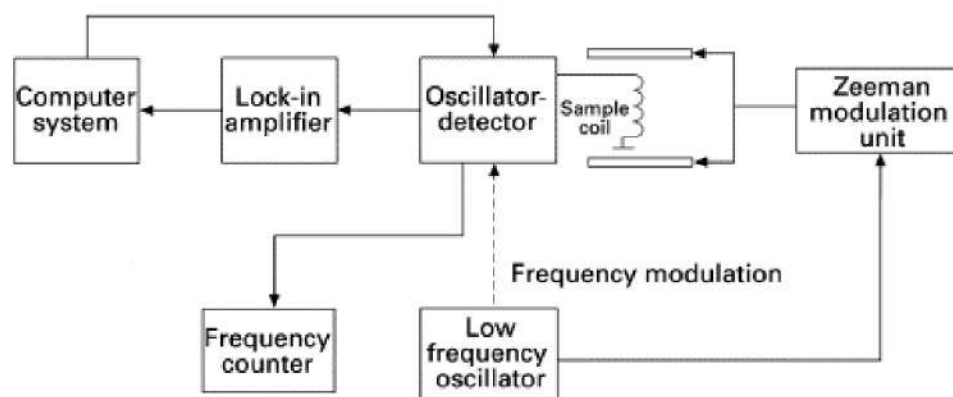
NQR methods typically have a better than 99% compound-specific detection rate and a false positive rate of less than 1% for very small amounts of plastic explosives.

INTERPRETATION AND CHEMICAL EXPLANATION OF NQR SPECTROSCOPY:

Nuclear quadrupole resonance spectroscopy or NQR is a chemical analysis technique related to nuclear magnetic resonance (NMR).^[1] Unlike NMR, NQR transitions of nuclei can be detected in the absence of a magnetic field, and for this reason NQR spectroscopy is referred to as "zero Field NMR." The NQR resonance is mediated by the interaction of the electric field gradient (EFG) with the quadrupole moment of the nuclear charge distribution.

Because the EFG at the location of a nucleus in a given substance is determined primarily by the valence electrons involved in the particular bond with other nearby nuclei, the NQR frequency at which transitions occur is unique for a given substance. A particular NQR frequency in a compound or crystal is proportional to the product of the nuclear quadrupole moment, a property of the

nucleus, and the EFG in the neighborhood of the nucleus. It is this product which is termed the nuclear quadrupole coupling constant for a given isotope in a material and can be found in tables of known NQR transitions.



In NMR, nuclei with spin $\geq 1/2$ have a magnetic dipole moment so that their energies are split by a magnetic field, allowing resonance absorption of energy related to the difference between the ground state energy and the excited state. In NQR, on the other hand, nuclei with spin ≥ 1 , such as ^{14}N , ^{17}O , ^{35}Cl and ^{63}Cu , also have an electric quadrupole moment so that their energies are split by an electric field gradient, created by the electronic bonds in the local environment.

This quadrupole moment is associated with non-spherical charge distribution, and is a measure of flatness or oblateness. Since unlike NMR, NQR is done in an environment without a static (or DC) magnetic field, it is sometimes called "zero field NMR". Many NQR transition frequencies depend strongly upon temperature.

Any nucleus with more than one unpaired nuclear particle (protons or neutrons) will have a charge distribution which results in an electric quadrupole moment. Allowed nuclear energy levels are shifted unequally due to the interaction of the nuclear charge with an electric field gradient supplied by the non-uniform

distribution electron density (e.g. from bonding electrons) and/or surrounding ions. As in the case of NMR, irradiation of the nucleus with a burst of RF electromagnetic radiation, if of a particular frequency, results in absorption of some energy by the nucleus which can be viewed as a perturbation of the quadrupole energy level.

Unlike the NMR case, NQR absorption takes place in the absence of an external magnetic field. Application of an external static field to a quadrupolar nucleus splits the quadrupole levels by the energy predicted from the Zeeman interaction. The technique is very sensitive to the nature and symmetry of the bonding around the nucleus. The energy level shifts are much larger than the chemical shifts measured in NMR. Due to symmetry, the shifts become averaged to zero in the liquid phase, so NQR spectra can only be measured for solids.

UNIT – V

ESR and Mossabauer Spectroscopy

ESR Spectroscopy : Basic Principles – Experiments – ESR Spectrometer – Reflection Cavity and Microwave Bridge – ESR Spectrum – Hyperfine Structure.

Mossabauer Spectroscopy : Mossabauer Effect – Recoilless Emission and Absorption – Dopplervelocity shift – Mossabauer Spectrum – Experimental Methods – Hyperfine Interaction – Chemical Isomer Shift– Magnetic Hyperfine and electric Quadrupole Interaction

BASIC PRINCIPLES OF ESR SPECTROSCOPY:

Electron paramagnetic resonance (EPR) or **electron spin resonance (ESR)** spectroscopy is a technique for studying materials with unpaired electrons. The basic concepts of EPR are analogous to those of nuclear magnetic resonance (NMR), but it is electron spins that are excited instead of the spins of atomic nuclei. Because most stable molecules have all their electrons paired, the EPR technique is less widely used than NMR. However, this limitation also means that EPR offers great specificity, since ordinary chemical solvents and matrices do not give rise to EPR spectra.

EPR was first observed in Kazan State University by Soviet physicist Yevgeny Zavoisky in 1944, and was developed independently at the same time by Brebis Bleaney at the University of Oxford. Electron Spin resonance spectroscopy is based on the absorption of microwave radiation by an unpaired electron when it is exposed to a strong magnetic field. Species that contain unpaired electrons

(namely free radicals, odd-electron molecules, transition metal complexes, rare earth ions, etc.) can therefore be detected by ESR.

The basic principles behind EPR are very similar to the more ubiquitous nuclear magnetic resonance spectroscopy (NMR), except that EPR focuses on the interaction of an external magnetic field with the unpaired electron(s) in a molecule, rather than the nuclei of individual atoms. EPR has been used to investigate kinetics, mechanisms, and structures of paramagnetic species and along with general chemistry and physics, has applications in biochemistry, polymer science, and geosciences.

The degeneracy of the electron spin states is lifted when an unpaired electron is placed in a magnetic field, creating two spin states, $m_s = \pm \frac{1}{2}$, where $m_s = -\frac{1}{2}$, the lower energy state, is aligned with the magnetic field. The spin state on the electron can flip when electromagnetic radiation is applied. In the case of electron spin transitions, this corresponds to radiation in the microwave range.

The energy difference between the two spin states is given by the equation

$$\Delta E = E_+ - E_- = h\nu = g\beta B$$

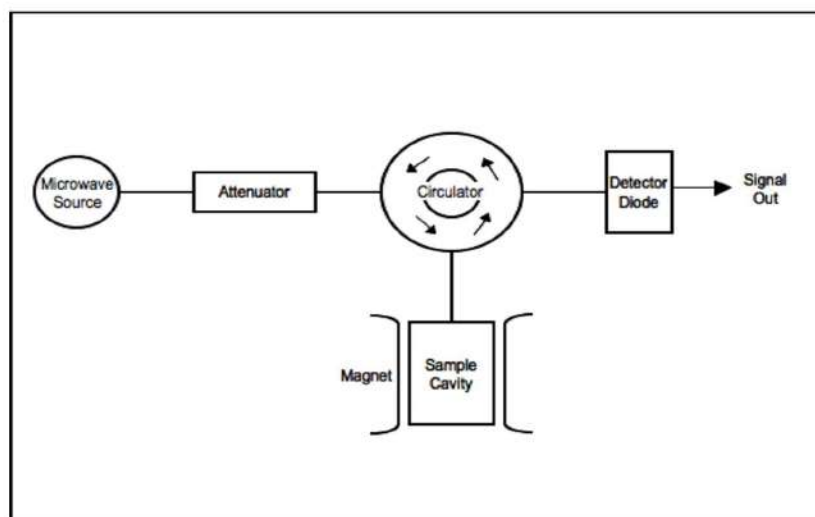
where h is Planck's constant ($6.626 \times 10^{-34} \text{ J s}^{-1}$), ν is the frequency of radiation, β is the Bohr magneton ($9.274 \times 10^{-24} \text{ J T}^{-1}$), B is the strength of the magnetic field in Tesla, and g is known as the g -factor. The g -factor is a unitless measurement of the intrinsic magnetic moment of the electron, and its value for a free electron is 2.0023. The value of g can vary, however, and can be calculated by rearrangement of the above equation, i.e.,

$$g = h\nu / \beta B$$

using the magnetic field and the frequency of the spectrometer. Since h , ν , and β should not change during an experiment, g values decrease as B increases. The concept of g can be roughly equated to that of chemical shift in NMR.

EXPERIMENTS OF ESR SPECTROSCOPY:

EPR spectroscopy can be carried out by either 1) varying the magnetic field or holding the frequency constant or 2) varying the frequency and holding the magnetic field constant (as is the case for NMR spectroscopy). Commercial EPR spectrometers typically vary the magnetic field and holding the frequency constant, opposite of NMR spectrometers. The majority of EPR spectrometers are in the range of 8-10 GHz (X-band), though there are spectrometers which work at lower and higher fields: 1-2 GHz (L-band) and 2-4 GHz (S-band), 35 GHz (Q-band) and 95 GHz (W-band).

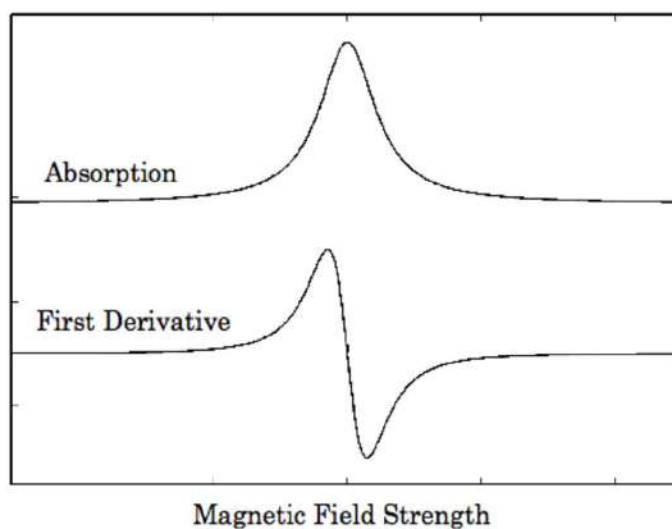


Block diagram of a typical EPR spectrometer.

EPR spectrometers work by generating microwaves from a source (typically a klystron), sending them through an attenuator, and passing them on to the sample, which is located in a microwave cavity (Figure). Microwaves reflected back

from the cavity are routed to the detector diode, and the signal comes out as a decrease in current at the detector analogous to absorption of microwaves by the sample. Samples for EPR can be gases, single crystals, solutions, powders, and frozen solutions. For solutions, solvents with high dielectric constants are not advisable, as they will absorb microwaves. For frozen solutions, solvents that will form a glass when frozen are preferable. Good glasses are formed from solvents with low symmetry and solvents that do not hydrogen bond. Drago provides an extensive list of solvents that form good glasses.

EPR spectra are generally presented as the first derivative of the absorption spectra for ease of interpretation. An example is given in Figure.



Example of first and second derivative EPR spectrum.

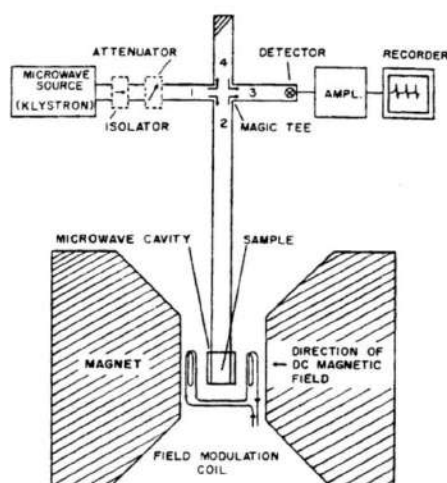
Magnetic field strength is generally reported in units of Gauss or mTesla. Often EPR spectra are very complicated, and analysis of spectra through the use of computer programs is usual. There are computer programs that will predict the EPR spectra of compounds with the input of a few parameters.

ESR SPECTROMETER:

Electron Spin resonance spectroscopy is based on the absorption of microwave radiation by an unpaired electron when it is exposed to a strong magnetic field. Species that contain unpaired electrons (namely free radicals, odd-electron molecules, transition metal complexes, rare earth ions, etc.) can therefore be detected by ESR.

WORKING PRINCIPLE:

When an atomic or molecular system with unpaired electrons is subjected to a magnetic field, the electronic energy levels of the atom or molecule will split into different levels. The magnitude of the splitting is dependent on the strength of the applied magnetic field. The atom or molecule can be excited from one split level to another in the presence of an external radiation of frequency corresponding to the frequency obtained from the difference in energy between the split levels.



Such an excitation is called magnetic resonance absorption. The atom or molecule under investigation may be in different environments in an actual sample.

The magnetic resonance frequency will hence be influenced by the local environment of the atom or molecule. The electron spin resonance technique is therefore, a probe for a detailed identification of the various atomic and molecular systems and their environments and all associated parameters.

APPLICATIONS:

Electron Spin Resonance, ESR, is a powerful non-destructive and non-intrusive analytical method. ESR yields meaningful structural information even from ongoing chemical or physical processes, without influencing the process itself. It is the ideal technique to complement other analytical methods in a wide range of application areas.

One can perform studies related to :

- Molecular structure
- Crystal structure
- Reaction kinetics
- Valence electron wave functions
- Molecular motion
- Relaxation properties
- Electron transport
- Crystal / ligand fields
- Reaction mechanisms etc.

REFLECTION CAVITY & MICROWAVE BRIDGE:

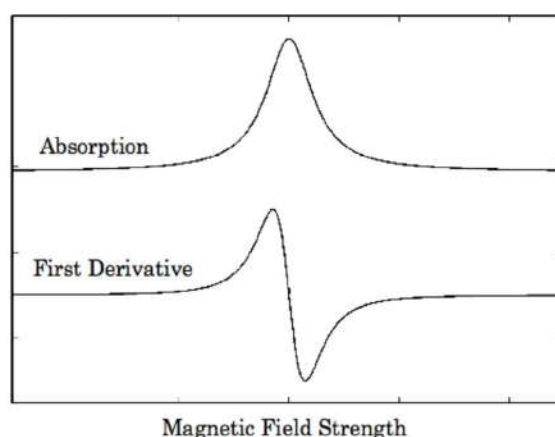
A **microwave cavity** or radio frequency (RF) cavity is a special type of resonator, consisting of a closed (or largely closed) metal structure that confines

electromagnetic fields in the microwave region of the spectrum. The structure is either hollow or filled with dielectric material.

A microwave cavity acts similarly to a resonant circuit with extremely low loss at its frequency of operation, resulting in quality factors up to the order of 10^6 , compared to 10^2 for circuits made with separate inductors and capacitors at the same frequency. They are used in oscillators and transmitters to create microwave signals, and as filters to separate a signal at a given frequency from other signals, in equipment such as radar equipment, microwave relay stations, satellite communications, and microwave ovens. In addition to their use in electrical networks, RF cavities can manipulate charged particles passing through them by application of acceleration voltage and are thus used in particle accelerators.

ESR SPECTRUM:

EPR spectra are generally presented as the first derivative of the absorption spectra for ease of interpretation. An example is given in Figure.



Example of first and second derivative EPR spectrum.

Magnetic field strength is generally reported in units of Gauss or mTesla. Often EPR spectra are very complicated, and analysis of spectra through the use of computer programs is usual. There are computer programs that will predict the EPR spectra of compounds with the input of a few parameters.

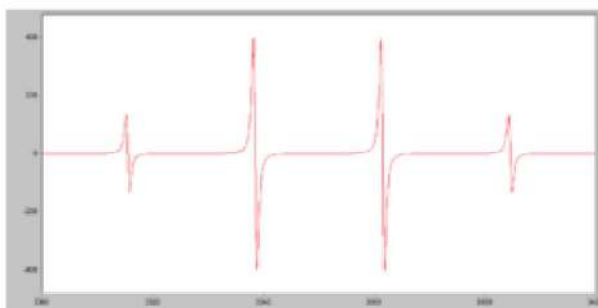
HYPERFINE STRUCTURE:

Since the source of an EPR spectrum is a change in an electron's spin state, it might be thought that all EPR spectra for a single electron spin would consist of one line. However, the interaction of an unpaired electron, by way of its magnetic moment, with nearby nuclear spins, results in additional allowed energy states and, in turn, multi-lined spectra. In such cases, the spacing between the EPR spectral lines indicates the degree of interaction between the unpaired electron and the perturbing nuclei. The hyperfine coupling constant of a nucleus is directly related to the spectral line spacing and, in the simplest cases, is essentially the spacing itself.

Two common mechanisms by which electrons and nuclei interact are the Fermi contact interaction and by dipolar interaction. The former applies largely to the case of isotropic interactions (independent of sample orientation in a magnetic field) and the latter to the case of anisotropic interactions (spectra dependent on sample orientation in a magnetic field). Spin polarization is a third mechanism for interactions between an unpaired electron and a nuclear spin, being especially important for π -electron organic radicals, such as the benzene radical anion. The symbols " a " or " A " are used for isotropic hyperfine coupling constants while " B " is usually employed for anisotropic hyperfine coupling constants.

In many cases, the isotropic hyperfine splitting pattern for a radical freely tumbling in a solution (isotropic system) can be predicted. For a radical having M equivalent nuclei, each with a spin of I , the number of EPR lines expected is $2MI + 1$. As an example, the methyl radical, CH_3 , has three ^1H nuclei each with $I = 1/2$, and so the number of lines expected is $2MI + 1 = 2(3)(1/2) + 1 = 4$, which is as observed.

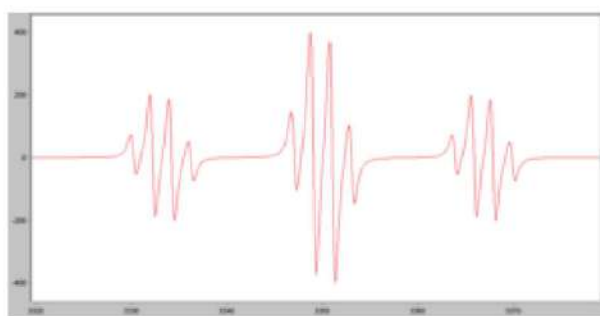
For a radical having M_1 equivalent nuclei, each with a spin of I_1 , and a group of M_2 equivalent nuclei, each with a spin of I_2 , the number of lines expected is $(2M_1I_1 + 1)(2M_2I_2 + 1)$. As an example, the methoxymethyl radical, $\text{H}_2\text{C}(\text{OCH}_3)$, has two equivalent ^1H nuclei each with $I = 1/2$ and three equivalent ^1H nuclei each with $I = 1/2$, and so the number of lines expected is $(2M_1I_1 + 1)(2M_2I_2 + 1) = [2(2)(1/2) + 1][2(3)(1/2) + 1] = [3][4] = 12$, again as observed.



Simulated EPR spectrum of the CH_3 radical

The above can be extended to predict the number of lines for any number of nuclei. While it is easy to predict the number of lines a radical's EPR spectrum should show, the reverse problem, unraveling a complex multi-line EPR spectrum and assigning the various spacings to specific nuclei, is more difficult.

In the oft-encountered case of $I = 1/2$ nuclei (e.g., ^1H , ^{19}F , ^{31}P), the line intensities produced by a population of radicals, each possessing M equivalent nuclei, will follow Pascal's triangle. For example, the spectrum at the right shows that the three ^1H nuclei of the CH_3 radical give rise to $2MI + 1 = 2(3)(1/2) + 1 = 4$ lines with a 1:3:3:1 ratio. The line spacing gives a hyperfine coupling constant of $a_{\text{H}} = 23 \text{ G}$ for each of the three ^1H nuclei. Note again that the lines in this spectrum are *first derivatives* of absorptions.



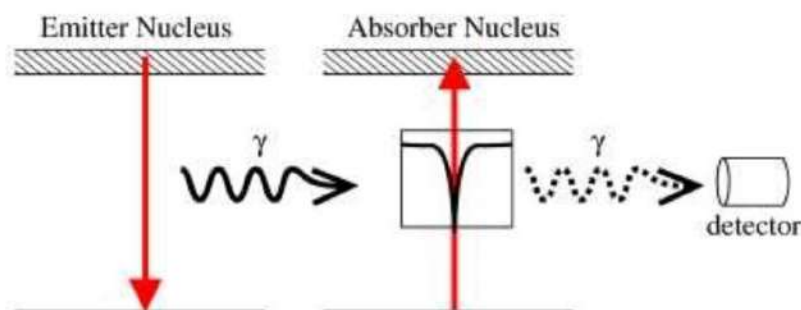
Simulated EPR spectrum of the $\text{H}_2\text{C}(\text{OCH}_3)$ radical

As a second example, consider the methoxymethyl radical, $\text{H}_2\text{C}(\text{OCH}_3)$. The two equivalent methyl hydrogens will give an overall 1:2:1 EPR pattern, each component of which is further split by the three methoxy hydrogens into a 1:3:3:1 pattern to give a total of $3 \times 4 = 12$ lines, a triplet of quartets. A simulation of the observed EPR spectrum is shown at the right, and agrees with the 12-line prediction and the expected line intensities. Note that the smaller coupling constant (smaller line spacing) is due to the three methoxy hydrogens, while the larger coupling constant (line spacing) is from the two hydrogens bonded directly to the carbon atom bearing the unpaired electron. It is often the case that coupling constants decrease in size with distance from a radical's unpaired electron, but there are some notable exceptions, such as the ethyl radical (CH_2CH_3).

MOSSBAUER SPECTROSCOPY:

It is a spectroscopic technique based on the Mössbauer effect. This effect, discovered by Rudolf Mössbauer in 1957, consists of the recoil-free, resonant absorption and emission of gamma rays in solids.

Like NMR spectroscopy, Mössbauer spectroscopy probes tiny changes in the energy levels of an atomic nucleus in response to its environment. Typically, three types of nuclear interactions may be observed: an isomeric shift, also known as a chemical shift; quadrupole splitting; and magnetic or hyperfine splitting, also known as the Zeeman effect. Due to the high energy and extremely narrow line widths of gamma rays, Mössbauer spectroscopy is a very sensitive technique in terms of energy (and hence frequency) resolution, capable of detecting change in just a few parts per 10.

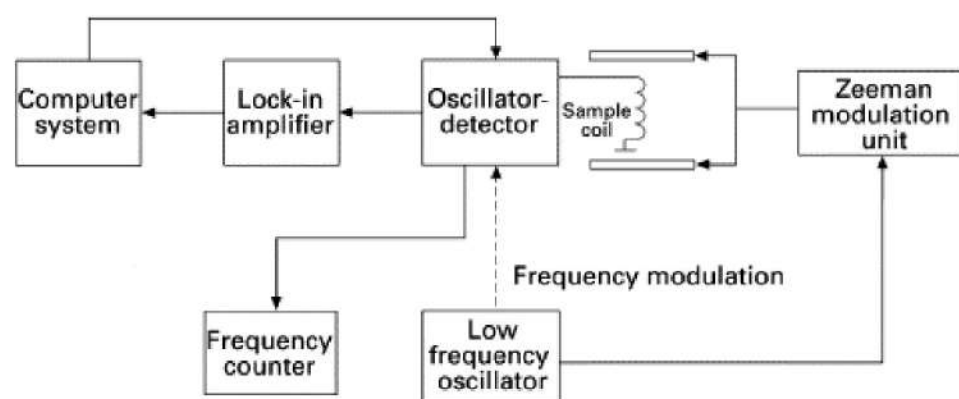


Us as a gun recoils when a bullet is fired, conservation of momentum requires a nucleus (such as in a gas) to recoil during emission or absorption of a gamma ray. If a nucleus at rest *emits* a gamma ray, the energy of the gamma ray is slightly *less* than the natural energy of the transition, but in order for a nucleus at rest to *absorb* a gamma ray, the gamma ray's energy must be slightly *greater* than the natural energy, because in both cases energy is lost to recoil. This means that nuclear resonance (emission and absorption of the same gamma ray by

identical nuclei) is unobservable with free nuclei, because the shift in energy is too great and the emission and absorption spectra have no significant overlap.

Nuclei in a solid crystal, however, are not free to recoil because they are bound in place in the crystal lattice. When a nucleus in a solid emits or absorbs a gamma ray, some energy can still be lost as recoil energy, but in this case it always occurs in discrete packets called phonons (quantized vibrations of the crystal lattice). Any whole number of phonons can be emitted, including zero, which is known as a "recoil-free" event. In this case conservation of momentum is satisfied by the momentum of the crystal as a whole, so practically no energy is lost.

Mossbauer found that a significant fraction of emission and absorption events will be recoil-free, which is quantified using the Lamb–Mössbauer factor.^[2] This fact is what makes Mössbauer spectroscopy possible, because it means gamma rays emitted by one nucleus can be resonantly absorbed by a sample containing nuclei of the same isotope, and this absorption can be measured.



MOSSBAUER EFFECT:

The **Mössbauer effect**, or **recoilless nuclear resonance fluorescence**, is a physical phenomenon discovered by Rudolf Mössbauer in 1958. It involves the

resonant and recoil-free emission and absorption of gamma radiation by atomic nuclei bound in a solid. Its main application is in Mössbauer spectroscopy.

In the Mössbauer effect the narrow resonance absorption for nuclear gamma absorption can be successfully attained by physically immobilizing atomic nuclei in a crystal. The immobilization of nuclei at both ends of a gamma resonance interaction is required so that no gamma energy is lost to the kinetic energy of recoiling nuclei at either the emitting or absorbing end of a gamma transition. Such loss of energy causes gamma ray resonance absorption to fail. However, when emitted gamma rays carry essentially all of the energy of the atomic nuclear de-excitation that produces them, this energy is also sufficient to excite the same energy state in a second immobilized nucleus of the same type.

The emission and absorption of x-rays by gases had been observed previously, and it was expected that a similar phenomenon would be found for gamma rays, which are created by nuclear transitions (as opposed to x-rays, which are typically produced by electronic transitions). However, attempts to observe nuclear resonance produced by gamma-rays in gases failed due to energy being lost to recoil, preventing resonance (the Doppler effect also broadens the gamma-ray spectrum). Mössbauer was able to observe resonance in nuclei of solid iridium, which raised the question of why gamma-ray resonance was possible in solids, but not in gases. Mössbauer proposed that, for the case of atoms bound into a solid, under certain circumstances a fraction of the nuclear events could occur essentially without recoil. He attributed the observed resonance to this recoil-free fraction of nuclear events.

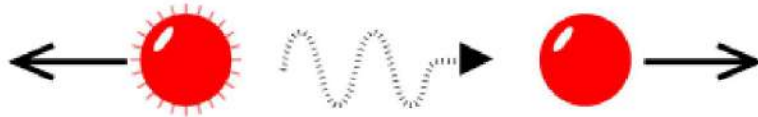
The Mössbauer effect was one of the last major discoveries in physics to be originally reported in German language. The first report in English language was a letter describing a repetition of the experiment. The discovery was rewarded with the Nobel Prize in Physics in 1961 together with Robert Hofstadter's research of electron scattering in atomic nuclei.

RECOIL EMISSION AND ABSORPTION:

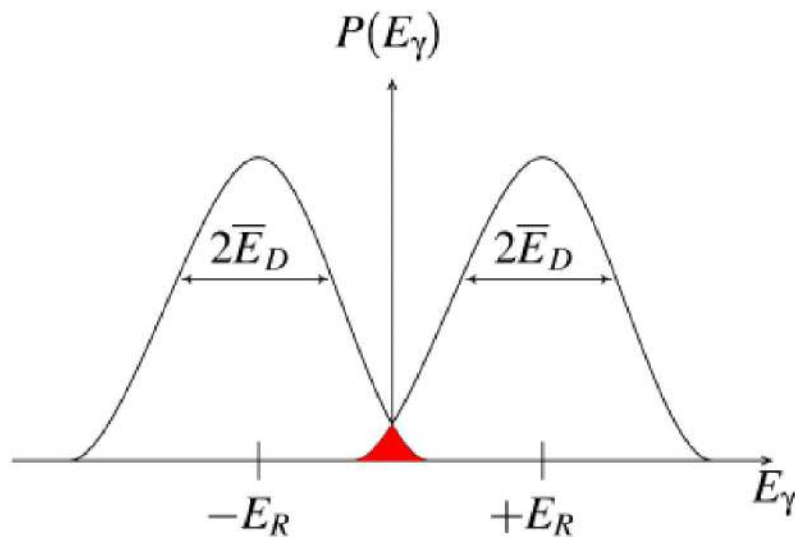
Nuclei in atoms undergo a variety of energy level transitions, often associated with the emission or absorption of a gamma ray. These energy levels are influenced by their surrounding environment, both electronic and magnetic, which can change or split these energy levels. These changes in the energy levels can provide information about the atom's local environment within a system and ought to be observed using resonance-fluorescence.

There are, however, two major obstacles in obtaining this information: the 'hyperfine' interactions between the nucleus and its environment are extremely small, and the recoil of the nucleus as the gamma-ray is emitted or absorbed prevents resonance.

In a free nucleus during emission or absorption of a gamma ray it recoils due to conservation of momentum, just like a gun recoils when firing a bullet, with a recoil energy E_R . This recoil is shown in Fig1. The emitted gamma ray has E_R less energy than the nuclear transition but to be resonantly absorbed it must be E_R *greater* than the transition energy due to the recoil of the absorbing nucleus. To achieve resonance the loss of the recoil energy must be overcome in some way.



As the atoms will be moving due to random thermal motion the gamma-ray energy has a spread of values E_D caused by the Doppler effect. This produces a gamma-ray energy profile as shown in Fig2. To produce a resonant signal the two energies need to overlap and this is shown in the red-shaded area. This area is shown exaggerated as in reality it is extremely small, a millionth or less of the gamma-rays are in this region, and impractical as a technique.



What Mössbauer discovered is that when the atoms are within a solid matrix the effective mass of the nucleus is very much greater. The recoiling mass is now effectively the mass of the whole system, making E_R and E_D very small.

If the gamma-ray energy is small enough the recoil of the nucleus is too low to be transmitted as a phonon (vibration in the crystal lattice) and so the whole system recoils, making the recoil energy practically zero: a recoil-free event. In this

situation, as shown in Fig3, if the emitting and absorbing nuclei are in a solid matrix the emitted and absorbed gamma-ray is the same energy: resonance!



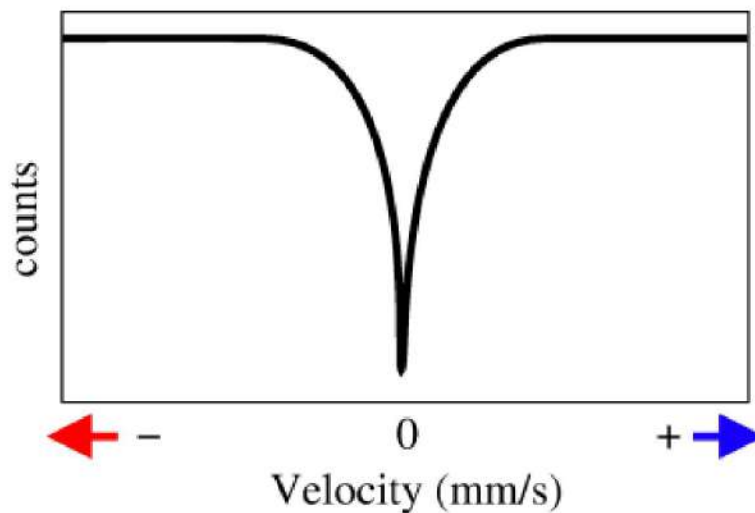
MOSSBAUER SPECTRUM:

So far we have seen one Mössbauer spectrum: a single line corresponding to the emitting and absorbing nuclei being in identical environments. As the environment of the nuclei in a system we want to study will almost certainly be different to our source the hyperfine interactions between the nucleus and the its environment will change the energy of the nuclear transition. To detect this we need to change the energy of our probing gamma-rays. This section will show how this is achieved and the three main ways in which the energy levels are changed and their effect on the spectrum.

As shown previously the energy changes caused by the hyperfine interactions we will want to look at are very small, of the order of billionths of an electron volt. Such miniscule variations of the original gamma-ray are quite easy to achieve by the use of the doppler effect. In the same way that when an ambulance's siren is raised in pitch when it's moving towards you and lowered when moving away from you, our gamma-ray source can be moved towards and away from our absorber.

This is most often achieved by oscillating a radioactive source with a velocity of a few mm/s and recording the spectrum in discrete velocity steps. Fractions of mm/s compared to the speed of light (3×10^{11} mm/s) gives the minute energy shifts

necessary to observe the hyperfine interactions. For convenience the energy scale of a Mössbauer spectrum is thus quoted in terms of the source velocity, as shown in Fig1.



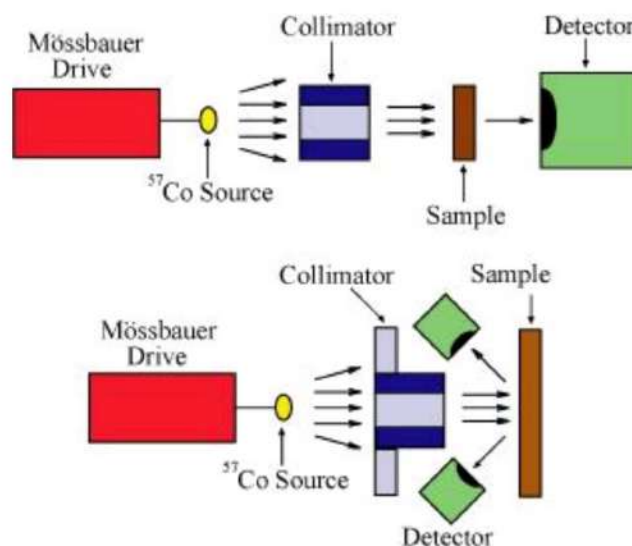
With an oscillating source we can now modulate the energy of the gamma-ray in very small increments. Where the modulated gamma-ray energy matches precisely the energy of a nuclear transition in the absorber the gamma-rays are resonantly absorbed and we see a peak. As we're seeing this in the transmitted gamma-rays the sample must be sufficiently thin to allow the gamma-rays to pass through, the relatively low energy gamma-rays are easily attenuated.

In Fig1 the absorption peak occurs at 0mm/s, where source and absorber are identical. The energy levels in the absorbing nuclei can be modified by their environment in three main ways: by the Isomer Shift, Quadrupole Splitting and Magnetic Splitting.

EXPERIMENTAL METHODS:

The basic elements of a Mössbauer spectrometer are a source, sample, detector, and a drive to move the source or absorber. Most commonly, this is done by moving the source toward and away from the sample, while varying velocity linearly with time. For example, for ^{57}Fe , moving the source at a velocity of 1 mm/sec toward the sample increases the energy of the emitted photons by about ten natural linewidths.

For simplicity, "mm/sec" is the conventional "energy" unit in Mössbauer spectroscopy. It is also possible to leave the source stationary and oscillate the sample, as is done with synchrotron Mössbauer. The location of the detector relative to the source and the sample defines the geometry of the experiment (Figure 5); most commonly, either transmission or backscatter modes are used.



HYPERFINE INTERACTION:

Mössbauer spectroscopy allows the researcher to probe structural elements of the nucleus in several ways, termed isomer shift, quadrupole interactions, and

magnetic splitting. These are each explained by the following sections as individual graphs, but in practice Mössbauer spectrum are likely to contain a combination of all effects.

CHEMICAL ISOMER SHIFT:

An isomeric shift occurs when non identical atoms play the role of source and absorber, thus the radius of the source, R_s , is different that of the absorber, R_a , and the same holds that the electron density of each species is different. The Coulombic interactions affects the ground and excited state differently leading to a energy difference that is not the same for the two species. This is best illustrated with the equation:

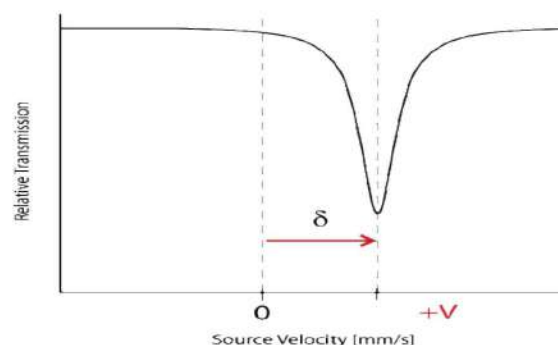
$$R_A \neq R_S$$

$$\rho_A \neq \rho_S$$

$$E_A \neq E_S$$

$$\delta = E_A - E_S = 23nZe^2(\rho_A - \rho_S)(R_{2e}^2 - R_{2g}^2)$$

Where delta represents the change in energy necessary to excite the absorber, which is seen as a shift from the Doppler speed 0 to V_1 . The isomer shift depends directly on the s-electrons and can be influenced by the shielding p,d,f electrons. From the measured delta shift there is information about the valance state of the absorbing atom.



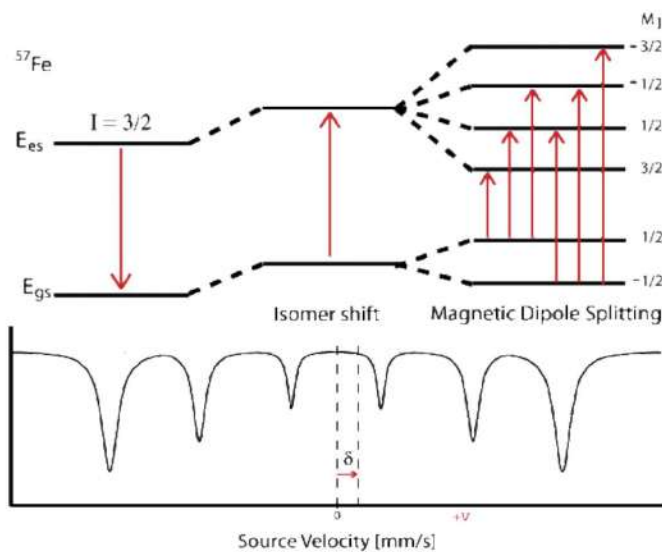
The energy level diagram for δ shift shows the change in source velocity due to different sources used. The shift may be either positive or negative.

MAGNETIC HYPERFINE INTERACTION:

Magnetic splitting of seen in Mössbauer spectroscopy can be seen because the nuclear spin moment undergoes dipolar interactions with the magnetic field

$$E(m_I) = -gn\beta_n B_{eff} m_I$$

where gn is the nuclear g -factor and β_n is the nuclear magneton. In the absence of quadrupole interactions the Hamiltonian splits into equally spaced energy levels of



The allowed gamma stimulated transitions of nuclear excitation follows the magnetic dipole transition selection rule:

$$\Delta I = 1 \text{ and } \Delta m_I = 0, \pm 1$$

M_i is the magnetic quantum number and the direction of β defines the nuclear quantization axis. If we assume g and A are *isotropic* (direction independent) where $g_x = g_y = g_z$ and B is actually a combination of the applied and internal magnetic fields:

$$H = g\beta S \cdot B + AS \cdot I - gn\beta n B \cdot I$$

The electronic Zeeman term is far larger than the nuclear Zeeman term, meaning the electronic term dominates the equation so S is approximated by $\langle S \rangle$ and

$$\langle S_z \rangle = m_s = \pm 1/2 \text{ and } \langle S_x \rangle = \langle S_y \rangle \approx 0$$

$$H_n = A \langle S \rangle \cdot I - gn\beta n B \cdot I$$

Pulling out a $-gn\beta n$ followed by I leaves

$$H_n = -gn\beta n (-A \langle S \rangle gn\beta n + B) I$$

Substituting the internal magnetic field with

$$B_{int} = -A \langle S \rangle gn\beta n$$

results in a combined magnetic field term involving both the applied magnetic field and the internal magnetic field

$$H_n = -gn\beta n (B_{int} + B) \cdot I$$

which is simplified by using the effective magnetic field B_{eff}

$$H_n = -gn\beta n B_{eff} \cdot I$$

ELECTRIC QUADRUPOLE INTERACTION:

The Hamiltonian for quadrupole interaction using ^{57}Fe nuclear excited state is given by

$$H_Q = eQV_{ZZ} \frac{1}{2} [3I_z^2 - I(I+1) + \eta(I_x^2 - I_y^2)]$$

where the nuclear excited states are split into two degenerate doublets in the absence of magnetic interactions. For the asymmetry parameter $\eta=0$ doublets are labeled with magnetic quantum numbers $m_{es} = \pm 3/2$ and $m_{es} = \pm 1/2$, where the $m_{es} = \pm 3/2$ doublet has the higher energy. The energy difference between the doublets is thus

$$\Delta E_Q = eQV_{zz} \frac{1}{2} [1 + \frac{2}{3}\eta] \sqrt{I(I+1)}$$

The energy diagram and corresponding spectrum can be seen as

